NONLINEAR RESPONSE OF PHOTOSENSITIVE MATERIALS

Sarah Yasir

School of Computing, Science and Engineering
University of Salford, Salford, UK

Submitted in Partial Fulfilment of the Requirements of the Degree of Master of Philosophy, September 2014

Abstract:

The knowledge of nonlinear properties of optical waveguides is of great importance for the communication devices. The properties of waveguide material depend on how the material responds to the applied optical field.

A programme of work was performed to determine the potential use of single mode optical fibres in communication devices. The non-linear response of the optical fibre core to the light guiding is reported. A brief introduction to the work done in the past was also included.

The origin of the parametric processes, classified as second-order or third-order processes depending on order of susceptibility, lies in the nonlinear response of a material to an applied optical field. The second-order susceptibility vanishes for an isotropic media such as silica fibres, however in practice these processes are reported to occur. Four-wave mixing in optical fibres has been studied extensively since it can be quite efficient in generating new waves.

The characteristics of different types of single mode optical fibres have been examined, including the high germanium fibre and the D-section fibre. The different non-linear processes including the second harmonic generation (SHG) and third harmonic generation (THG), the four-wave mixing (FWM) and the other photo induced changes in the optical fibre were investigated. The effect of hydrogen diffusion was also studied in order to enhance the SHG efficiency. It has been found that careful diffusion of Hydrogen into the optical fibre core enhances the second harmonic generation process. The vital characteristics of colour centres in the optical fibres are explored and their contribution in the nonlinear response is studied. A number of different techniques have been explored and a number of different experimental methods have been adopted and developed. Finally suggestions for further development have been made.

Table of Contents

List of Figures

Chapter 2

Chapter 3

Chapter 4

Chapter 1

Introduction:

1.1 Introduction

The photo-sensitivities in the optical fibres and the factors behind this photosensitivity have been studied in this project. The objective of this study was to look into the factors causing the nonlinear effects in the optical fibres. The high intensity radiation exposure, mainly from the laser source affects some important optical fibre parameters like refractive index etc and the calculation of these parameters before and after the exposure to these radiations are used to measure the photosensitivity of the optical fibres.

The nonlinear optics is an important part of physics which was developed with the introduction of light amplification by stimulated emission of radiation, laser. With the beginning of nonlinear optics the production of new frequencies took place by multi-wave mixing of various frequencies in nonlinear mediums.

This chapter summarises general processes involved in a laser system. It aims at the fundamental basics of lasers such as the excitation system, laser cavity dimensions, basic concepts of absorption, emission, population inversion and amplification phenomenon.

The nonlinear effects especially second harmonic generation, studied in the past and different studies done to find the origins of the nonlinear effects are explained in chapter 2. Some theoretical explanation of the process is also included. The observation of some other effects such as four-wave mixing is also discussed along with some explanation.

In chapter 3 the experimental work done to investigate the nonlinear effects is described. The second harmonic generation and other wavelengths observed are explained. The nonlinearities are studied in different types of optical fibres.

Mono-chromator calibration and the measurement of numerical aperture of the different optical fibres are included in chapter 4. Effects of diffusion of hydrogen in silica are also described in chapter 4.

In chapter 5 the work done on photo-chromic glasses is explained with the help of fourier optics.

1.2 The Basics of Laser

The basic laser system comprises of an excitation system, laser cavity dimensions, basic concepts of absorption, emission, population inversion and amplification phenomenon. Since the arrival of laser it has found various uses such as in microsurgery, compact-disc players, communications, holography, for drilling holes in hard materials and alignment in tunnel drilling.

1.2.1 Absorption and Emission:

According to quantum mechanics, the electrons can only have certain values of energy which are represented by energy levels. The more distant electrons from the nucleus have the higher values of energy. When an electron absorbs a photon of light, it is excited to the upper energy level and stays in this excited state for a period of time approximately 10^{-6} seconds and then it returns to its previous energy level emitting a photon of light.

1.2.2 Stimulated Emission:

When an atom exists in the excited state, the emission process can be triggered by its interaction with another photon. In this case the outcome is two photons, one the originally absorbed photon and the other photon stimulating the emission process. Although this process is very uncommon normally. A high number of atoms in the excited state are needed for the stimulated emission to take place. This situation is known as population inversion.

1.2.3 Population Inversion:

The population inversion is a compulsory condition for laser radiation to be produced. The first material found suitable for this process was synthetic ruby.

The intense burst of light from the xenon filled flash tubes is used to illuminate. The energy of electrons raises from the ground state to one of the broad band levels and then immediate shift takes place to two metastable levels without emission of light. The metastable levels have a longer life compared to the rest. This long life allows most of the electrons to stay in the excited state and hence resulting in the population inversion.

1.2.4 Light Amplification:

An amplifying medium is needed to increase the intensity of light passing through it. In Nd: YAG laser a rod of yttrium aluminium garnate (YAG) including neodymium ions is used as an amplifying medium. In HE: Ne laser a mixture of helium and neon gases is used as the amplifying medium. A thin layer of semiconductor material surrounded by two other semiconductor layers is used as an amplifying medium in the laser diode.

The intensity of light is increased by a factor called "Gain", while passing through the amplifying medium. This gain not only depends upon the energy of the amplifying medium but also on the wavelength of the incoming light and the length of the medium. For a high gain the amplifying medium must contain the sufficient energy which must be fed into the medium, this is termed as "pumping".

1.3 Optical fibres

There are numerous different types of optical fibres which have been used in different applications and are developed according to these applications. Various types of optical fibres with different characteristics are developed using different materials such as rare-earth material, non-silica glass and high germanium fibres. Different fabrication methods are also applied to construct these different fibres. The optical fibres are very popular in communications because unlike the common problem in copper wires, the light propagating through an optical fibre is not influenced by the external interference.

1.3.1 Structure of Optical fibres:

The optical fibres are cylindrical waveguides made up of a dielectric material such as fused silica mostly glass. The optical fibre consists of three concentric cylindrical layers, innermost is the core surrounding it is cladding and then the outermost protective coating. Light is guided through the core and cladding helps keeping light guided through the core. Whereas coating does not play any part in light propagation, it is included to protect fibre from environment dust etc. Refractive index of core material is kept higher than cladding material because of this difference in refractive index, light wave entering the fibre remains confined in the core due to total internal reflection at core/cladding interface.

The optical fibres are of two types, single mode optical fibres or multimode optical fibres. Single mode optical fibres have been used in this study. The single mode fibre have very small core diameter consisting of a few wavelengths. It has only one acceptable ray path for each frequency that is why light travels in single mode.

1.3.2 Photosensitivity in Optical fibres:

Any process taking place in the optical fibre depends on the material response as well as the wave guiding. Material properties depend on the material that optical fibre is made up of and can be enhanced by diffusion of some gases for example hydrogen. Wave guiding properties include mode pattern, phase matching and mode overlapping. These depend on the type of radiations passing through optical fibre.

Photosensitivity in the optical fibres was discovered in 1978. After that a lot of work and research has been done to investigate the phenomena. Some defects have been found to be present in the glass structure. During the glass formation some defects or impurities known as dopants are included in the glass structure, which interrelates with the vibration and electronic excitations of the glass, and results in the optical absorption. Most optical fibres function in the near infrared region. The low loss and optically linear optical fibres are found to display significant induced losses and second order nonlinearities that are otherwise forbidden under the influence of high intensity laser radiations.

The light induced modulation of a medium parameter like refractive index or attenuation coefficient gives rise to nonlinear response. This type of process is called parametric process and one such process is the second harmonic generation in optical fibres. The nonlinear optical coefficients have also been observed to change under the effect of laser radiations. The second harmonic at 532nm was observed after long period of intense Q-switched and mode-locked Nd: YAG laser radiation exposure at 1064nm. This was proposed to be a phase-matching process; a $\chi^{(2)}$ grating was suggested and later confirmed by measurements to be the reason behind the phenomenon. It was suggested that electronic polarisation takes place that originates the self alignment or organisation of the dopants or the defect centres found in

the glass material and this theory has been largely approved. A small quantity of green light was added to the laser radiations at fundamental wavelength and seeded into the core of optical fibre. This resulted in reduced preparation time reducing it to minutes rather than hours.

Various studies were undertaken to find out about the origins of this phenomenon. The defects in the optical fibre play a crucial part. Also a spatial charge field gives rise to induced second-order susceptibility. The $\chi^{(2)}$ phenomena were not expected to take place in optical fibres because of the presence of inversion symmetry. Because of which these $\chi^{(2)}$ phenomenon like second harmonic generation and three-photon parametric amplification have gained more attention than the $\chi^{(3)}$ phenomenon taking place in the optical fibres. These $\chi^{(3)}$ phenomena include spectral broadening, stimulated Raman and Brillouin scattering, nonlinear switching and four-wave mixing. The higher order terms such as magnetic dipoles and electric quadrupole have shown to give rise to some feeble second harmonic in optical fibres. Some very weak green light from long samples of optical fibres has been noticed. Some third harmonic light is also been reported in optical fibres. Later on conversion efficiency as high as 5% was reported in short length of optical fibre samples.

References:

1. P. N. Butcher and D. Cotter; The elements of nonlinear optics; Cambridge university press, 1990.
2. A. Yariv; Optical electronics in modern communications, fifth edition, Oxford Uni press, 1997.
3. G. Keiser; Optical fibre communications, McGraw-Hill, Inc, USA, 1991.
4. K. O. Hill., Y. Fuji, D. C. Johnson, B. S. Kawasaki; Photosensitivity of optical fibre waveguides; applications to reflection filter fabrication, Appl. Phys. Lett., 32, 647-649,1978.
5. U. Osterberg and W. Margulis; Dye laser pumped by Nd: YAG laser pulses frequency doubled in a glass optical fibre, Opt. Lett., 11, 516-518, 1986.
6. E. J. Friebele, D. L. Griscom, and G. H. Sigel; Defect centres in a germanium-doped silica-core optical fibre, J. Appl. Phys., 45, 3424-3428, 1974.
7. V. A. Kuzmenko; On the physical nature of the photon mixing processes in nonlinear optics, arXiv: physics/0102038 v 1, 2001.
8. J. W. Fleming; Material dispersion in light guide glasses, Electron Letters, 14, 326-328, 1978.
9. E. J. Friebele, D. L. Griscom and G. H. Sigel; Defect centres in a germanium-doped silica optical fibre, Journal of Applied Physics, 45, 3424-3429, 1974.
10. A. S. L. Gomes, U. Österberg and J. R. Taylor; Spectral and temporal investigations of nonlinearities in a non-polarization preserving single-mode optical fibre, App. Phys. B. 41, 235-240, 1986.
11. F. P. Kapron, D. B. Keck and R. D. Maurer; Radiation losses in glass optical waveguides, Applied Physics Letters, 17, 423-425, 1970.

Chapter 2

Nonlinear wave mixing

2.1 Introduction

The optical fibre core possesses microscopic inversion symmetry, which forbids second order contributions and hence optical fibre was not considered for producing second harmonic generation (SHG) until late eighties [1]. In 1987 however Österberg and Margulis reported SHG in optical fibres with 5 % efficiency for 1.06 μm. Different models have been used to understand the process since then. These models include mixing models, asymmetric photo-ionization model and destructive photo-orientation model.

2.2 SHG observed in Past

In the optical fibres SHG has been observed for a range of lengths ranging from shorter than 50 cm to longer than 1.5 km. It is established that some preparation process is involved in producing frequency doubling. The preparation process is described as the process of illuminating the fibre samples with high level laser radiations for some time interval. After a preparation time of a few minutes to a few hours SHG is produced [3]. SHG levels are not affected by interruption in the preparation period, levels are observed to be same on resumption.

The SHG efficiency increases exponentially with time for a constant infrared input power. The second harmonic green light is a quadratic function of input infrared in most cases where input levels are low i. E. < 10 kW.

The length dependence of SHG has been studied in the past [2], results obtained show that only a limited length of fibre is transformed during the preparation process to produce SHG and it also been shown that a major amount of SHG is produced near the input end.

The mode of SH green light has been recognised as LP_{11} mode in most cases [3]. Although other modes including LP_{01} mode have also been observed in some cases. SHG has been observed in different types of optical fibres with different efficiencies. SHG conversion efficiency of 3×10^{-6} has been observed for poled silicate fibres at 1kw infrared pump powers [6]. For rare earth doped alluminosilicate fibres second harmonic conversion efficiency of 1.5 % has been achieved at 200 w infrared peak powers [5]. By in diffusion of hydrogen followed by heating, SH efficiency has been observed to enhance by a factor of 4.4 [4]. The saturation magnitude of $\chi^{(2)}$ varies with choice of proper glass dopant and fibre fabrication process [4]. SH light saturates quicker for short lengths samples of fibres than the longer fibre samples [7].

2.2.1 The $\chi^{(2)}$ grating

A number of studies have taken place to find out the origin of this frequency doubling mechanism and the effect has been attributed to the periodic $\chi^{(2)}$ grating produced along the fibre upon illumination with high input powers [8]. The grating formed during preparation process is assumed to be permanent dipole allowed $\chi^{(2)}$ grating. The $\chi^{(2)}$ grating is presumed to be the result of rearrangement of colour centres along the fibre. The colour centres are rearranged to provide the periodicity for phase matching the second harmonic process [8].

The formation of periodic grating in fibre upon illumination was studied and direct images of these gratings were taken by etching the fibres as shown in fig(2.1) [10]. The optical fibres were etched using hydrofluoric acid, the grating period was thereby found. It was observed that any differences in phase velocities of fundamental and second harmonic light can be adjusted by the grating period. The experimental results contradicted the earlier mentioned assumption that grating results from "macroscopic orientation of dipoles throughout the material" [8]. They believe that the grating results from macroscopic separation of charge at boundary between the fibre core and cladding, the spectral width of grating has been found to be 0.24nm [11].

2.2.2 SHG a Quadrupole Process

Further studies show that second harmonic signal is produced at half the coherence length [6]. SHG conversion efficiency can be improved by adjusting the coherence length of $\chi^{(2)}$ grating [12]. Moreover it has been suggested that SHG is more likely to be the result of a quadrupole process rather than a dipole process as thought earlier and it's shown by experiments [9]. Spatially periodic electric field is produced in fibre as a result of photoelectron emission occurs as direct consequence of interference between multiphoton absorption processes [13]. Second harmonic light is produced because of dc electric field in fibre which provides the requirement for phase matching. It is supposed that charge redistribution takes place among the defect

centres following photo ionization by multiphoton processes also shown in fig (2.2) [13].

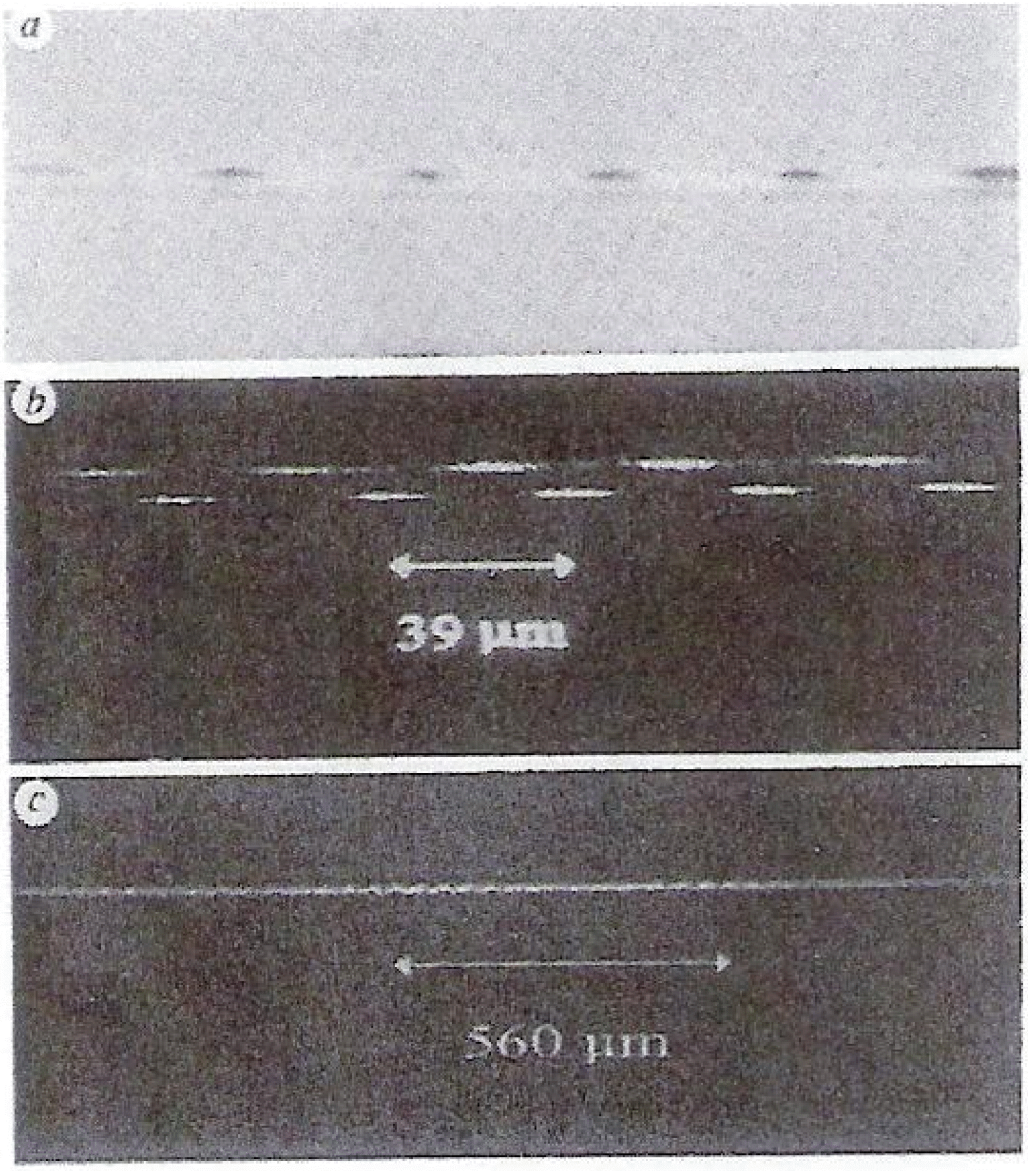

Fig 2.1: reference [10] The second order nonlinear $\chi^{(2)}$ gratings in optical fibres revealed by chemical exposure.

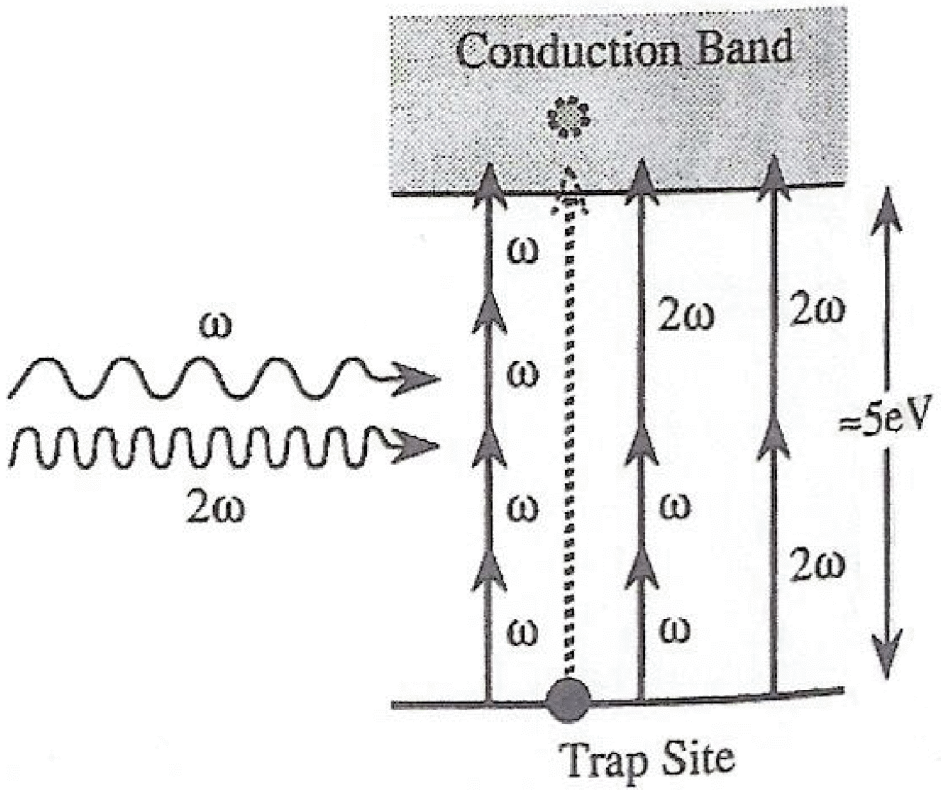

Fig 2.2: reference [13] Multiphoton paths to ionization, assuming a broad defect band at approximately 5 eV and a fundamental laser wavelength of 1.064 μm.

The photo ionization of an atom by two frequency field is shown as

$$E_{real}(r,t) = E_1 Cos(\omega t - \phi_1) + E_2 Cos(2\omega t - \phi_2)$$

Where $E_1 = E_2 = 1$

And $\Delta\phi = \phi_2 - 2\phi_1 = \frac{\pi}{4}$ [17]

Ionization potential of an atom $\hbar\omega_o$ should be such as $\hbar\omega < \hbar\omega_o < 2\hbar\omega$, in order for laser field E_1 to produce only two photon ionization and second harmonic field E_2 to produce only one photon ionization.

A strong transverse dc electric field acts on the allowed $\chi^{(3)}$ nonlinearity of the fibre, giving rise to an effective $\chi^{(2)}$. A photoinduced effect is considered to be the cause of dipole allowed second-order susceptibility [14].

$$P(0) = \varepsilon_0 \chi^{(3)}(0;\omega,\omega,-2\omega)E(\omega)E(\omega)E^*(2\omega)$$

A dc polarization is formed when a third order susceptibility acts on pump and second harmonic frequency at the phase matching periodicity which orients the defects. Thus phase matching condition is met and the permanently written periodic nonlinearity results in effective SHG within the fibre [14]. It is been established that in diffusion of hydrogen results in enhanced SHG. This is because OH content in fibre is increased by diffusion of hydrogen, which in turn gives rise to changed defect concentration, resulting in enhanced SHG [15]. $\chi^{(2)}$ is stated to be inversely proportional to Ge (3) defect concentration in germanium doped silica fibres [15].

2.3 Conditions necessary for SHG

For the second-order induced susceptibility the SHG process is represented by

$$P(2\omega) = E_0 \chi^{(2)}(2\omega, \omega, \omega) E(\omega) E(\omega)$$

To achieve efficient SHG, the beam at doubled frequency 2ω needs to be phase-matched to the fundamental beam at ω. This phase matching conservation requirement is represented as $k_{2\omega} = k_{\omega}$ or $n_{2\omega} = n_{\omega}$

In the presence of a grating

$$k_{2\omega} = 2k_{\omega} + K$$

These two steps need to be going inside the core of the fibre contributing to efficient second harmonic generation, schematically represented as in figure (2.3).

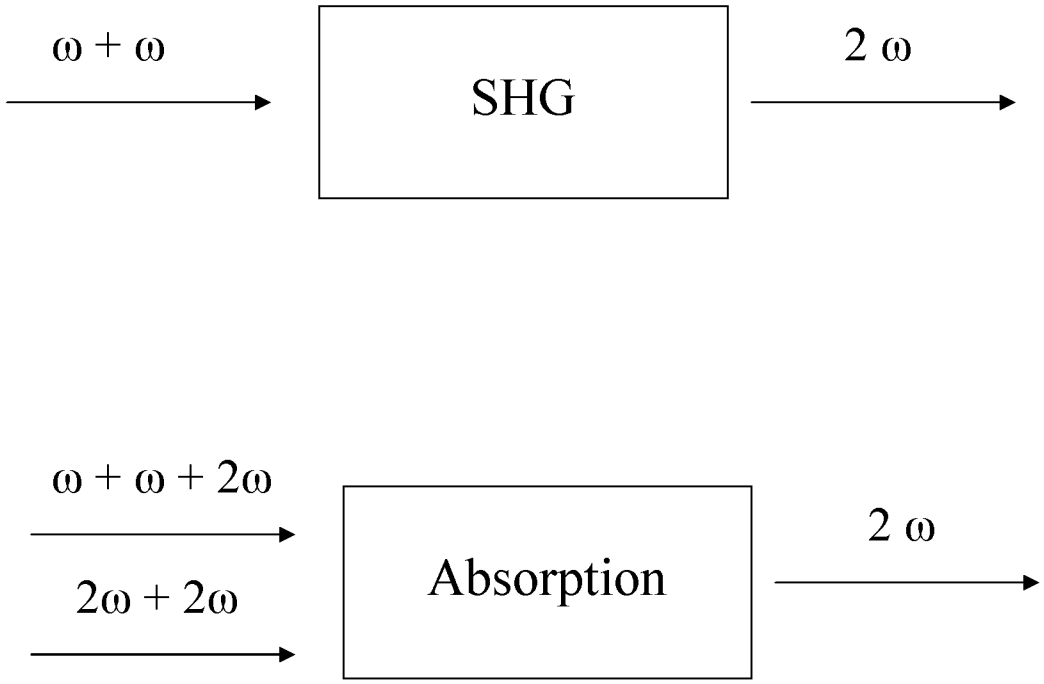

Fig 2.3: The two steps to give efficient SHG

The first step is SHG where two photons at the fundamental frequency 1064 nm combine to form one photon at twice the frequency. The next step is phase-matching where two photons at twice the fundamental frequency or two photons at fundamental frequency and one at twice the fundamental frequency are absorbed to excite an electron as a result of which we get the green light at 532 nm.

2.4 Theoretical Explanation of the Process

A first order susceptibility $\chi^{(1)}$ might be the reason for second harmonic generation inside the core of optical fibre. As it is the linear susceptibility, it will obviously have higher value than higher order susceptibilities $\chi^{(2)}$, $\chi^{(3)}$ etc. The nonlinear susceptibility is very low in magnitude as compared to linear susceptibility.

Even-wave mixing processes are actually allowed in centro-symmetric materials like optical fibres while odd-wave mixing processes are not allowed. So even-wave mixing processes might be more dominating than odd-wave mixing processes inside the optical fibres.

This suggests that instead of a $\chi^{(2)}$ nonlinearity a $\chi^{(3)}$ susceptibility can be the reason for observed frequency doubling process.

In the case that $\chi^{(3)}$ susceptibility is responsible for frequency doubling, third harmonic generation (a four-wave mixing process) of the fundamental frequency can occur as expressed following.

$$P(3\omega) = \varepsilon_0 \chi^{(3)}(3\omega;\omega,\omega,\omega)E(\omega)E(\omega)E(\omega)$$

The resulting frequency combines with the fundamental to produce second harmonic frequency.

$$P(2\omega) = \varepsilon_0 \chi^{(3)}(2\omega;3\omega,\omega,-2\omega)E(\omega)E(\omega)E^*(3\omega)$$

It can be represented by the following equations

$$\omega + \omega + \omega \rightarrow 3\omega$$
$$3\omega + \omega \rightarrow 2\omega + 2\omega$$

And schematically

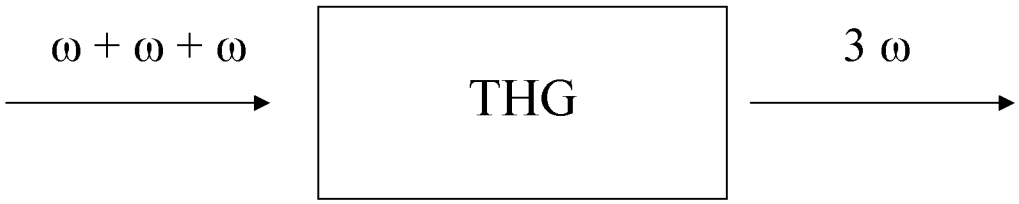

And

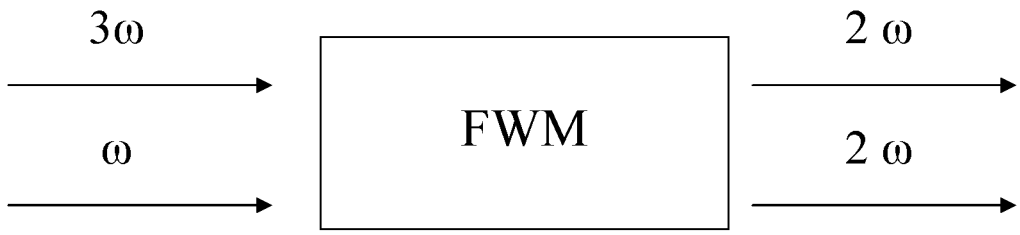

Fig 2.4: The two steps to give efficient SHG

2.4.1 Grating Formation

This process is not generally phase matched but can be phase matched if a grating is formed inside the core of the optical fibre and that is possible only if absorption takes place as shown in fig (2.10) and fig (2.11).

No definite evidence of the absorption process described above, exists however four-wave mixing process have been observed in significant amount in spectra as shown in diagrams (2.5, 2.6, 2.7 and 2.8) recorded from irradiated samples of the optical fibres. Some of the peaks in these spectra are quite sharp, comparable to the peak at second harmonic wavelength.

2.4.2 Explanation of the 647 nm Peak

The intense peak at 647 nm has also been seen in the past and was attributed to as four-wave mixing mechanism with the fundamental frequency acting as the pump wave. It had similar efficiency as SHG [9] as shown in figure (2.9).

$$2\omega_{1.064\mu m} \rightarrow \omega_{647nm} + \omega_{3.0017nm}$$

Visible red light has also been observed in 630 nm to 647 nm spectral range [2]. There are some additional lines forming a band-like spectrum around 532 nm and 647 nm peaks. These radiations appearing on spectrum of light by laser irradiation of the optical fibres were regarded as parasitic nonlinear processes imposing limitations on the second harmonic conversion efficiency. These lines around 532 nm can be explained as Stoke's shift of 532 nm or the second harmonic of some Stoke's shifts of the fundamental 1.064 μm wavelength. The details with the 647 nm peak in the spectrum are described as possibly due to four-photon mixing process with one of the Raman lines acting as the pump [9].

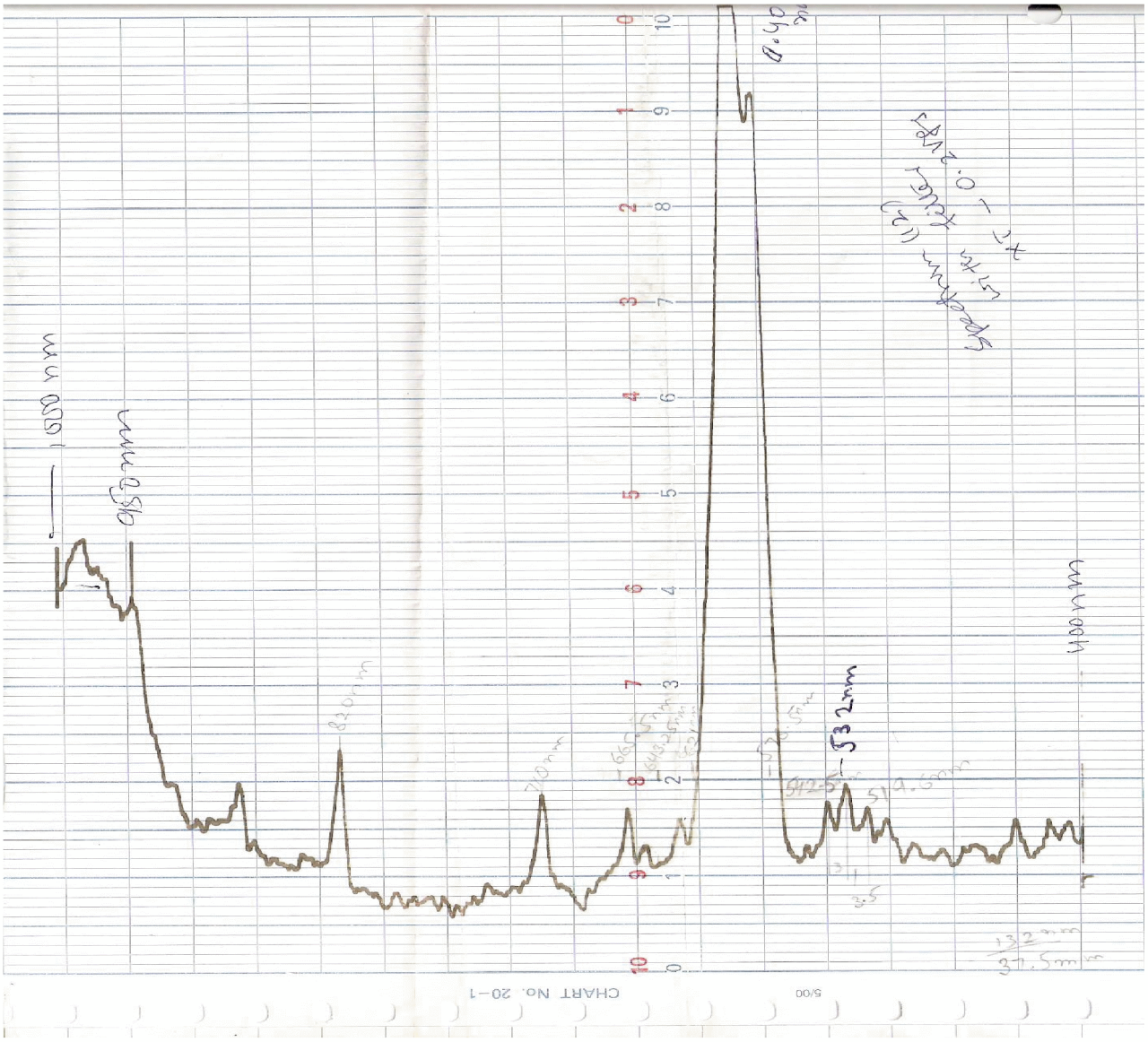

Fig (2.5): The high germanium optical fibre spectrum for the range 400nm to 1000nm for 1.06 µm pump radiation

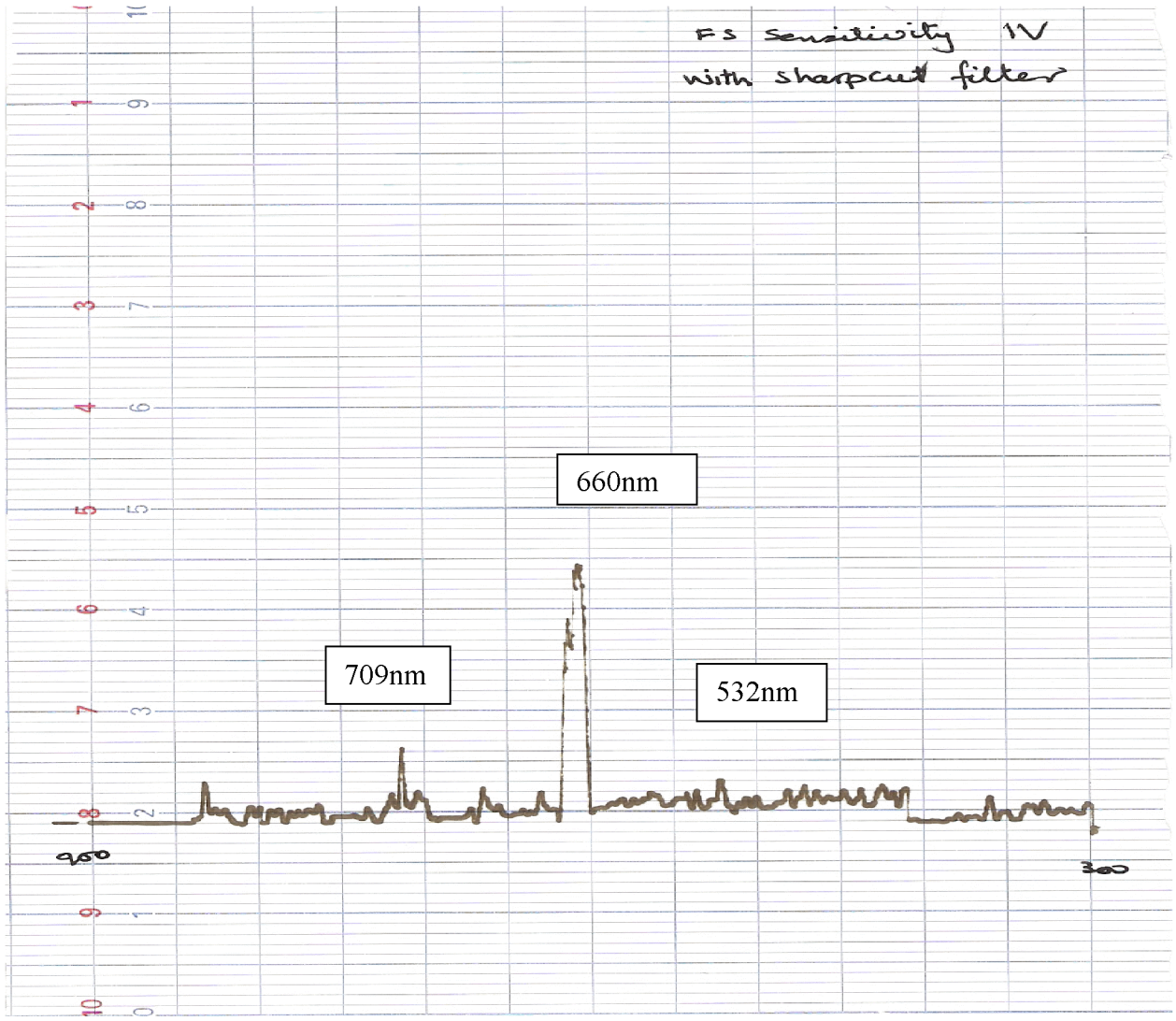

Fig (2.6): The > 1.5 km fibre sample spectrum for the range 300nm to 900nm for 1.06 µm pump radiation

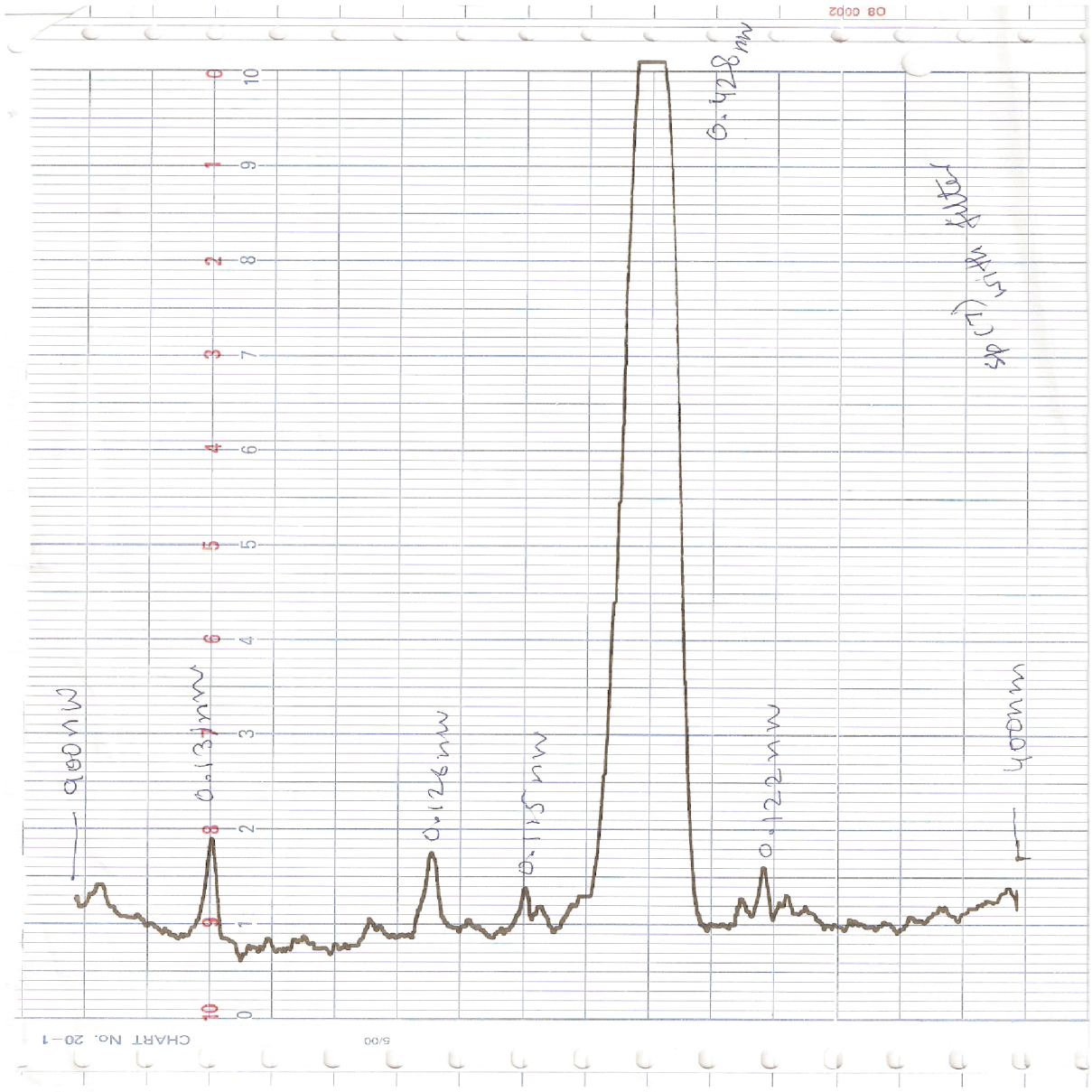

Fig (2.7): The optical fibre spectrum for the range 400nm to 900nm for 1.06 µm pump radiation

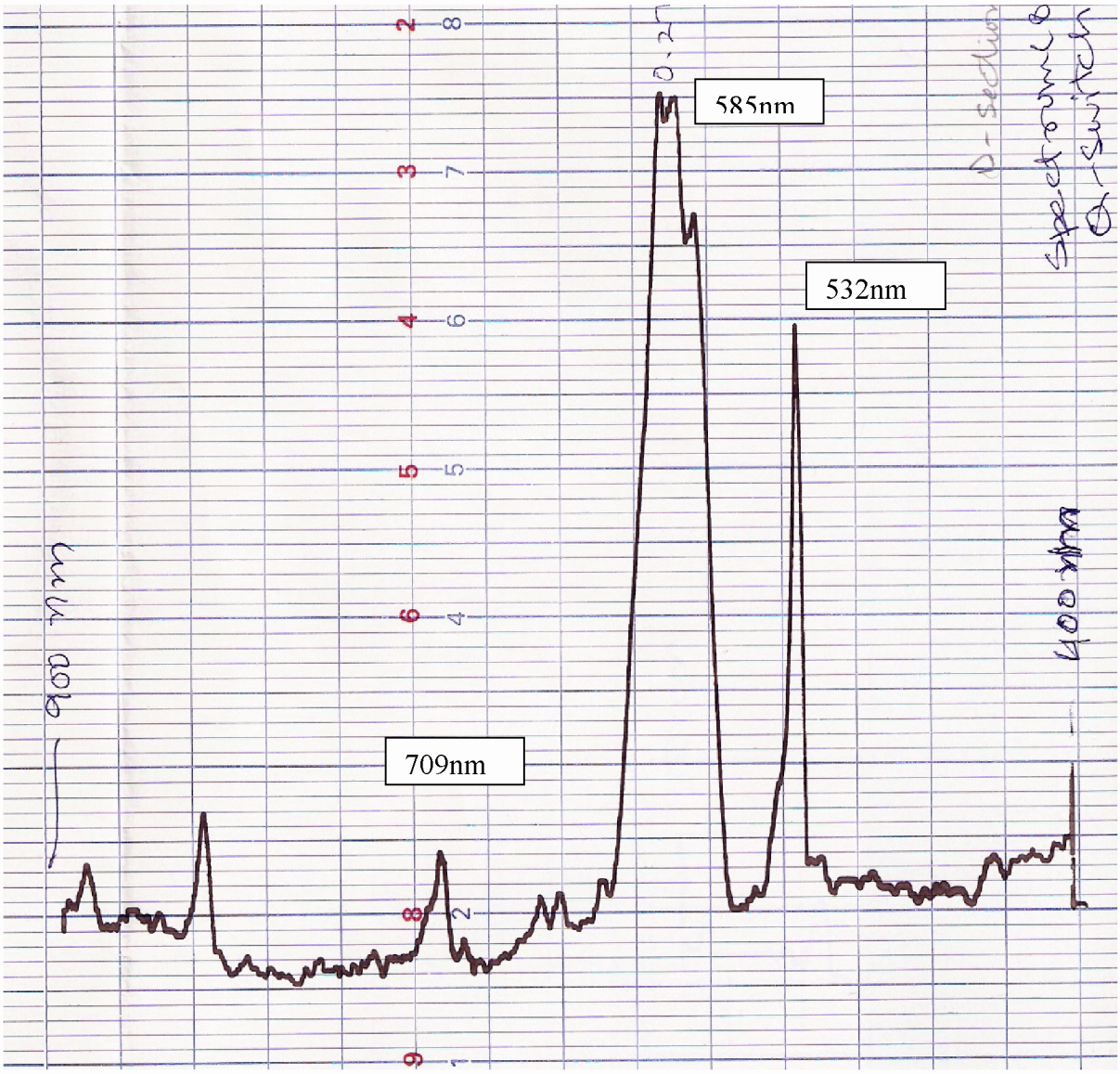

Fig (2.8): The D-section optical fibre spectrum for the range 400nm to 900nm for 1.06 µm pump radiation

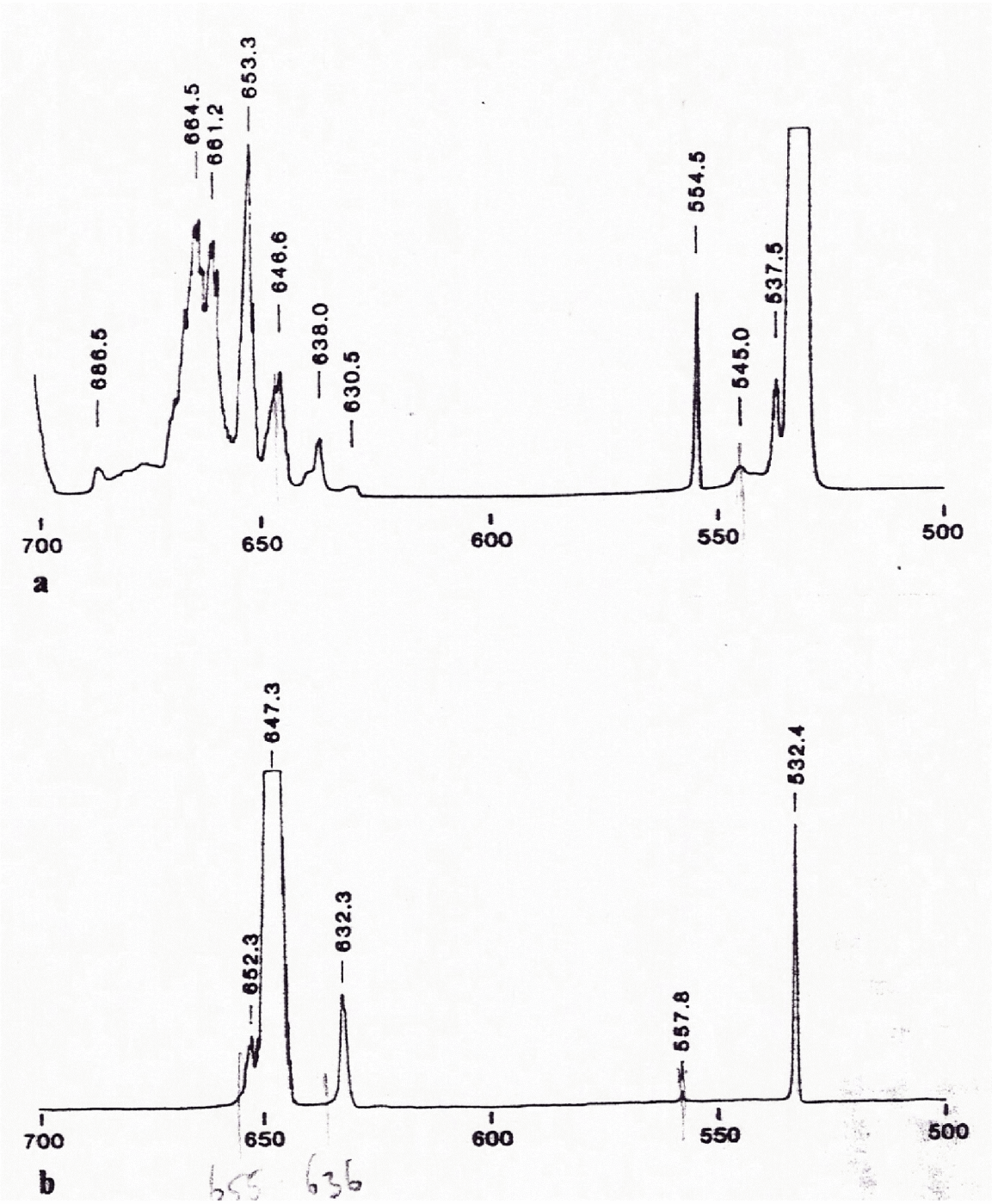

Fig (2.9): Reference [9] The generated spectra in the 500-700nm range for (a) 120 m and (b) 1.5 km fibre length.

2.4.3 Explanation of the Other Peaks

Other four-wave mixing wavelengths 355 nm, 585 nm, 709 nm and 820 nm are also observed in spectra as shown in figures (2.5, 2.6, 2.7 and 2.8). To explain the 355 nm wavelength three fundamental frequency photons can combine by a first order susceptibility $\chi^{(1)}$ (-3ω; ω, ω, ω) to form one photon at thrice the fundamental frequency as shown in figure (2.12) and as follows

$$\omega + \omega + \omega \rightarrow 3\omega$$

To give 709 nm at the output either one fundamental frequency photon combine with one twice the frequency photon $\chi^{(3)}$(-3/2ω; ω, 2ω, -3/2ω) as given by equation

$$\omega + 2\omega \rightarrow {}^{3}\!/_{2}\,\omega + {}^{3}\!/_{2}\,\omega$$

Or one thrice the frequency photon gives two 3/2 ω photons $\chi^{(1)}$(-3/2ω; 3ω, -3/2ω)

$$3\omega \rightarrow {}^{3}\!/_{2}\,\omega + {}^{3}\!/_{2}\,\omega$$

Both of these expected processes are shown in diagram (2.13).

The 851 nm peak in the spectrum can be a result of one ω and one 3/2 ω photon combining by $\chi^{(3)}$(-5/4ω; ω, 3/2ω, -5/4ω) as given as follows and in diagram (2.14).

$$\omega + {}^{3}\!/_{2}\,\omega \rightarrow {}^{5}\!/_{4}\,\omega + {}^{5}\!/_{4}\,\omega$$

The 608 nm peak can be a result of combination of one 2ω and one ω photon or it can result from combination of one 2ω photon and one 3/2 ω photon as shown below and given in diagram(2.15).

$$\omega + 2\omega \rightarrow {}^{7}\!/_{4}\,\omega + {}^{5}\!/_{4}\,\omega$$

Or

$$2\omega + {}^{3}\!/_{2}\,\omega \rightarrow {}^{7}\!/_{4}\,\omega + {}^{7}\!/_{4}\,\omega$$

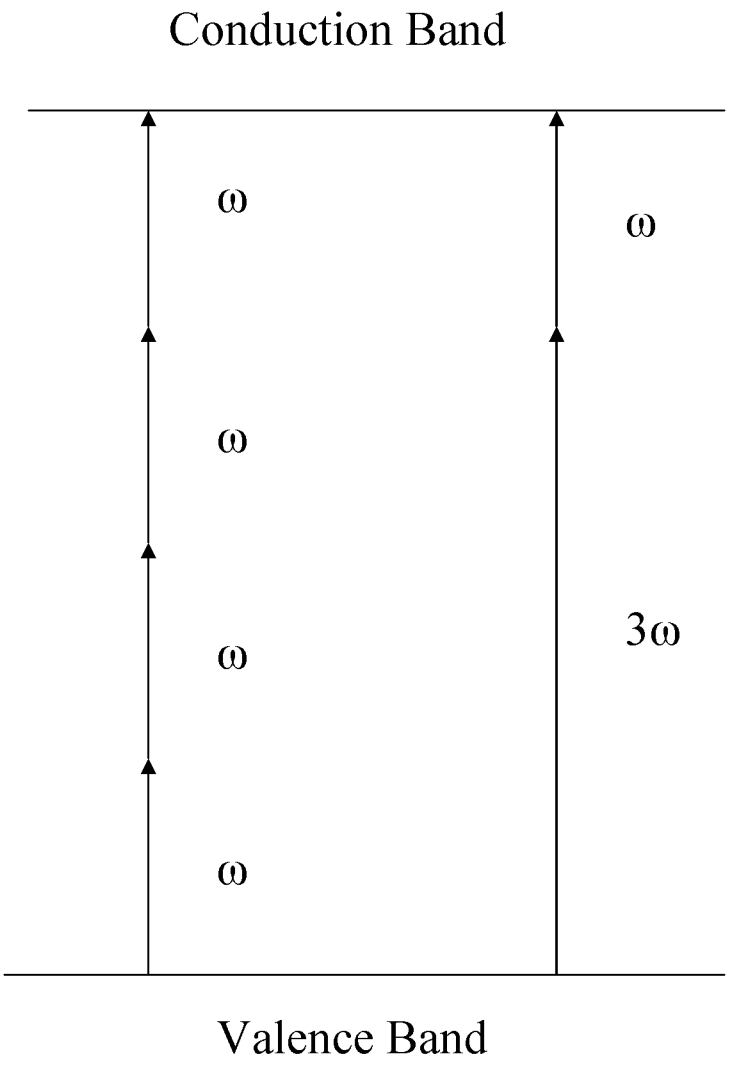

Fig 2.10: Absorption process to give efficient THG

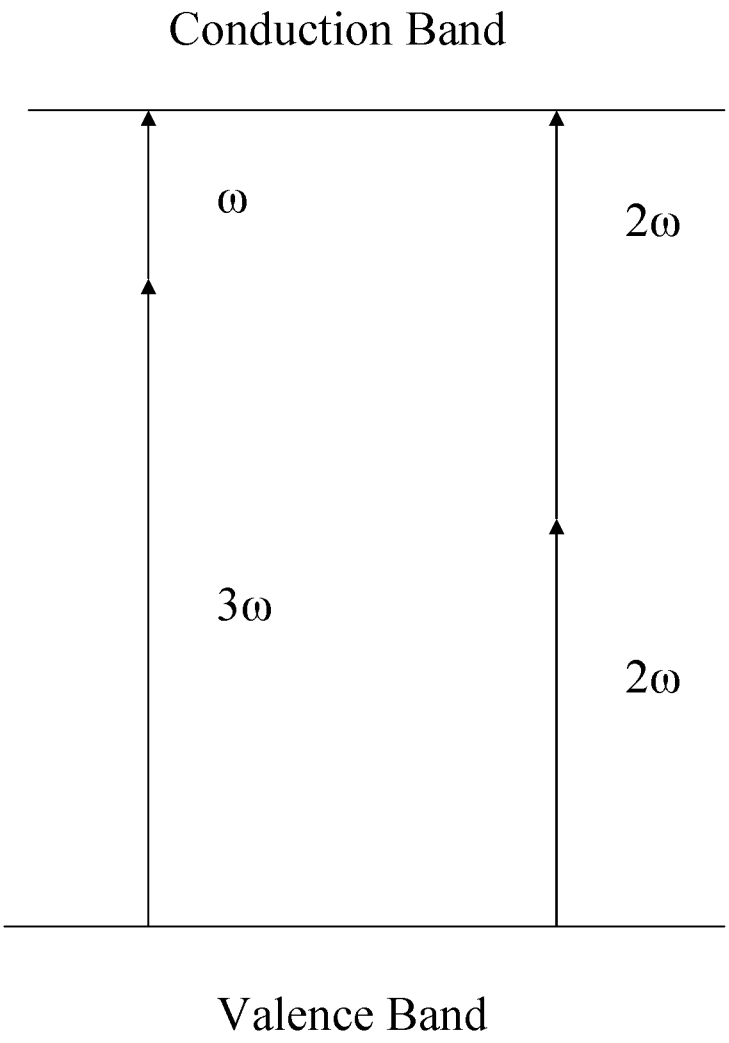

Fig 2.11: Absorption process to give efficient SHG

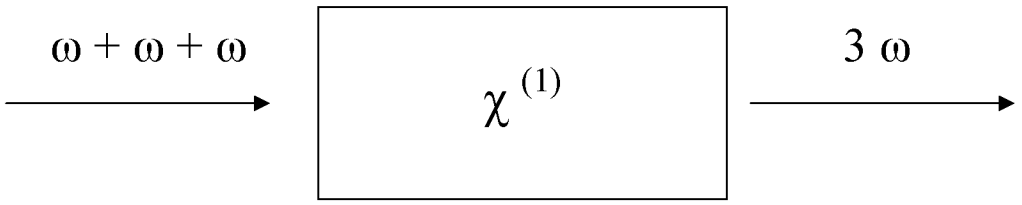

Fig 2.12: The step to give efficient THG

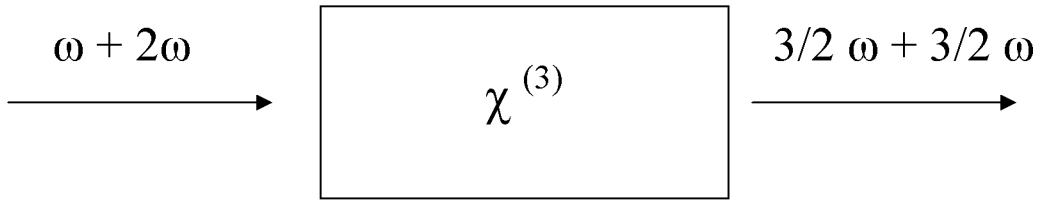

OR

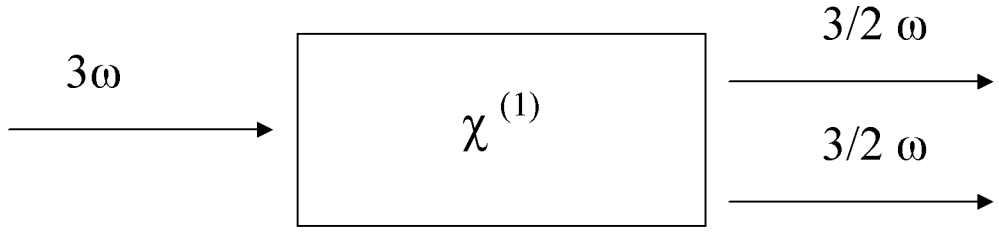

Fig 2.13: The two processes that give 3/2 ω

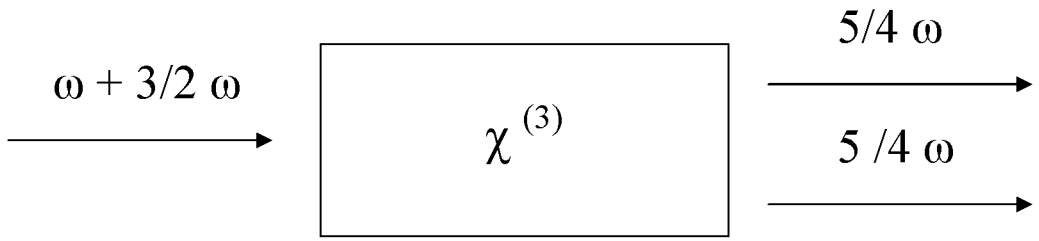

Fig 2.14: The step to give efficient 5 /4 ω

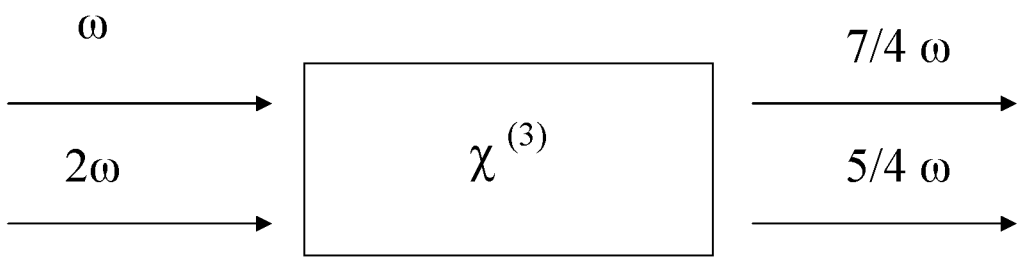

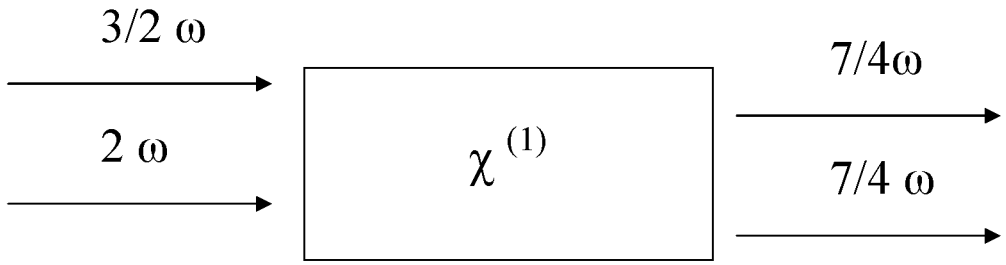

Fig 2.15: The process to give efficient 7/4 ω

References:

1. P. N. Butcher and D. Cotter; The elements of nonlinear optics; Cambridge university press, 1990.
2. A. Yariv; Optical electronics in modern communications, fifth edition, Oxford Uni press, 1997.
3. R. W. Boyd; Nonlinear Optics, London, Academic Press Limited, 1992.
4. F. G. Smith and T. A. King; Optics and Photonics, John Wiley and sons Ltd, Chichester England, 2000.
5. A. J. Francis and E. W. Harvey; Fundamental of optics, fourth edition, Mcgraw-hill Internation Edition, 1981.
6. R. Tilley; Color and the optical properties of materials, John Willey and sons Ltd, 2000.
7. U. Österberg and W. Margulis; Experimental studies on efficient frequency doubling in glass optical fibres, Opt. Lett. 12, 57, 1987.
8. U. Österberg and W. Margulis; Opt. Lett. 11, 516, 1986.
9. F. Ouellette, K. O. Hill and D. C. Johnson; Enhancement of second harmonic generation in optical fibres by a hydrogen and heat treatment, Appl. Phys. Lett. 54 (12), 1086, 1989.
10. F. Ouellette, D. Gagnon and M. Poirrier; Permanent photoinduced birefringence in a Ge-doped fibre, 58, 1813, 1991.
11. D. M. Krol and J. R. Simpson; Photoinduced second-harmonic generation in rare-earth-doped aluminosilicate optical fibers, Opt. Lett. 16 (21), 1650, 1991.
12. P. G. Kazansky, L. Dong and P. St. J. Russel; High second-order nonlinearities in poled silicate fibres, University of Southampton, 1994.
13. B. Batdorf, C. Krautschik, U. Österberg, G. Stageman, J. W. Leitch, J. R. Rotge and T. F. Morse; Study of the length dependence of frequency-doubled light in optical fibres, Opt. Comm. 73, 393, 1989.
14. H. W. Tom, R. H. Stolen, G. D. Aumiller and W. Peibel; Preparation of long-coherence-length second-harmonic-generating optical fibers by using mode-locked pulses, Opt. Lett. 13 (6), 512, 1988.

15. A. S. L. Gomes, U. Österberg and J. R. Taylor; Spectral and temporal investigations of nonlinearities in a non-polarization preserving single-mode optical fibre, App. Phy. B. 41, 235-240, 1986.
16. W. Margulis, F. Laurell and B. Lesche; Imaging the nonlinear grating in frequency-doubling fibres, Letters to nature. 378, 1995.
17. M. C. Farries, P.st. T. Russel, M.E. Fermann and D. N. Payne; Electrons Lett. 23, 322, 1987.
18. R. H. Stolen and W. K. Tom; Opt. Lett. 12, 585, 1987.
19. D. Z. Anderson, V. Mizrahi and J. E. Sipe; Model for second-harmonic generation in glass optical fibres based on asymmetric photoelectron emission from defect sites, Opt. Lett. 16, 796, 1991.
20. B.Valk, E. M. Kim and M. M. Salour; Second harmonic generation in Ge-doped fibres with a mode-locked Kr^{+} Laser, Appl. Phys. Lett. 51 (10), 722, 1987.
21. H. Itoh, Y.Ohmori and M. Nakahara; J. Lightwave Technol. Lt 4, 116, 1986.
22. N. B. Baranova and B.Y. Zel'dlovich; Physical effects in optical fields with nonzero average cube, $< E^3 > \neq 0$ J. Opt. Joc. Am B. 8 (1), 27, 1991.
23. M. Li, N. Zeng, C.Z.Shi, M. Zhang and Y. B. Liao; Fibre bragg grating distributed strain sensing: An adaptive simulated annealing algorithm approach, Optics & Laser Technology 37, 454, 2005.
24. S. Somekh and A. Yariv; Phase matching by periodic modulation of the nonlinear optical properties, Opt. Comm. 6, 301, 1972.
25. D. L. Nicacio, E. A. Gouveia, N. M. Borges and A. S. Gouveia; Third-harmonic generation in GeO_2-doped silica single-mode optical fibres, Appl. Phy. Lett. 62, 2179, 1993.
26. M. V. D. Vermelho, A. M. Reis, E. A. Gouveia, M. L. Lyra and A. S. Gouveia; Efficient frequency upconversion of 1.319μm radiation into intense yellow light at 580nm in pure SiO_2 core monomode optical fibre, Optics Lett. 18, 1496, 1993.
27. M. V. D. Vermelho, D. L. Nicacio, E. A. Gouveia and A. S. Gouveia; Efficient frequency upconversion of 1.064μm and 1.139μm Nd:YAG laser pulses into intense visible light in silica-based optical fibres, J. Opt. Soc. Am. B, 10, 1820, 1993.

28. M. Gallagher and U Osterberg; Time resolved 3.10ev luminescence in germanium doped silica glass, Appl. Phy. Lett. 63, 2987, 1993.
29. E. Snitzer; Cylindrical dielectric waveguide modes, J. opt. Soc. America, 51, 491, 1960.
30. A. Bhatti, H. S. Al-raweshidy and G. Murtaza; Polymer-coated D-fibre intended for electric field sensing, Fibre and integrated optics, 19, 79-85, 2000.
31. R. P. Depaula; Interaction of high frequency acoustic waves and optical waves propagating in single mode fibre, PhD Thesis, School of engineering, Catholic university of America, Washington, 1982.
32. A. D. Heaney, T. Erdogan and N. Borrelli; The significance of oxygen-deficient defects to the photosensitivity of hydrogen-loaded germane-silicate glass, J. Appl. Phys., 85, 7573-7578, 1999.
33. K. S. Lee and T. Erdogan; Mode coupling in spiral fibre gratings, Elect. Lett., 37, 156-157, 2001.
34. S. Jaswani, P. Sen and H. Mehta; Second harmonic generation in step index optical fibres, Pure Appl. Opt., 5, 71-76, 1996.
35. A. S. Furman; Photo induced bragg grating formation in optical fibres as a consequence of convective instability, Opt. Comm., 117, 502-506, 1995.
36. B. Poumellec; Nonlinear optical generations in silica-based optical fibres: material aspects, Opt. Mat., 3, 169-180, 1994.
37. G. Demouchy; Second harmonic generation in optical fibres, Experimental study of the self organised holographic grating length, Opt. Comm., 101, 5-6, 391-396, 1993.
38. D. D. Keck, R. D. Maurer, and P. C. Schultg; On the ultimate lower limit of attenuation in glass optical waveguide, Appl. Phys. Lett., 22, 307-309, 1973.
39. D. P. Hand and P. St. J. Russell; Solitary thermal shock waves and optical damage in optical fibres: The Fibre Fuse, Opt. Lett., 13, 767-769, 1998.
40. K. O. Hill, Y. Fuji, D. C. Johnson and B. S. Kawasaki; Photosensitivity of optical fibre wveguide;applications to reflection filter fabrication, Appl. Phys. Lett., 32, 647-499, 1978.
41. R. J. Potton, Poling of optical fibres using a frequency doubled argon laser, Lasers for Science Facility-Physics, Central Laser Facility Annual Report 2000/2001.

42. M. C. Farries, P. ST. Russell, M. E. Fermann and D. N. Payne; Second harmonic generation in an optial fibre by self-written $\chi^{(2)}$ grating, Electron Letters, 23, 322-324, 1987.
43. K. O. Hill, B. Malo, F. Bilodeau, D. C. Johnson and J. Albert; Bragg grating fabricated in monomode photosensitive optical fibre by UV exposure through a phase mask, Applied Physics Letters, 62, 1035-1037, 1993.

Chapter 3

Second Harmonic Generation

3.1 Introduction

In this chapter, the experimental setup for the second harmonic generation and results obtained are discussed. Experiments have been done using the optical fibre samples consisting different numerical apertures, core concentration of germanium and different fabrication processes. Different lengths of the optical fibre were used ranging from 20cm to about 1.5km.

3.2 Experimental Description

A Q-switched and mode-locked Quantronix 117 Nd: YAG laser was used to carry out experiments at 1.06 μm and 1.319μm wavelength. The mode-locked pulses were 90-100 ps and had 85 MHz repetition rate. The Q- Switch envelope width was 220 ns with a rate of 2 kHz. Another laser used was Q- switched Quantronix 114 Nd: YAG laser carry out experiments at 1.06μm to find out SHG and any other nonlinear processes occurring in optical fibre core.

3.2.1 Quantronix 117 at 1.06 μm

A Q-switched and mode-locked Quantronix 117 Nd: YAG laser was used to carry out experiments at 1.06 μm. The Mode-locked pulses were 90-100 ps and had 85 MHz repetition rate. The Q- Switch envelope width was 220 ns with a rate of 2 kHz. A 20X microscope objective lens was used to launch radiations into the fibre. A KTP crystal was used to produce second harmonic green light at 532 nm which along with infrared from laser was launched into the fibre sample using a 20 × microscope objective. The experimental setup used was as shown in fig (3.1). The fibre samples ranging from 20cm to about 60cm in length were used in experiments. The coating was stripped from the input and output ends of fibre for about 2 mm, and both ends were cut with a precision cutting tool for better launching. The fibre sample was mounted on a three axis fibre positioner. A Schott 3mm thick sharp cut filter with 850nm cut off wavelength was used to remove 532 nm radiations from the fibre input occasionally to allow only infrared into the sample fibre measure any second harmonic produced by optical fibre only. The green radiations and the infrared radiations at the output of optical fibre were guided through a plastic fibre of about 6 meters length into the power meter. Plastic optical fibre was used to get rid of all the infrared radiation from fibre output prior to entering the power meter so that only the output radiations coming from optical fibre other than the input infrared

radiations could be detected. The plastic optical fibre was chosen because of its high attenuation for infrared radiations. It had a loss of 14 dB/m at 1064 nm and 0.8dB/m at 532 nm. The output from fibre was monitored using a power meter; sometimes a mono-chromator, oscilloscope and an xt plotter were also used. The xt plotter was used to get the plot of readings with time at different stages. At a later time a monochromator was added in the experimental setup. Now the output of plastic fibre was focused into the monochromator using microscope objectives and the power meter was connected to the output of monochromator. A dc motor was used to tune monochromator to different wavelengths, to study the power of output form optical fibre at different wavelengths.

3.2.2 Quantronix 117 at 1.319 μm

A Q-switched and mode-locked Quantronix 117 Nd: YAG laser was used to carry out experiments at 1.319 μm. The mode-locked pulses were 90-100 ps and had 85 MHz repetition rate. The Q- Switch envelope width was 220 ns with a rate 2 kHz. A 20X microscope objective lens was used to launch radiations into the fibre. A KTP crystal was used to produce second harmonic green light at 660nm which along with infrared from laser was launched into the fibre sample using a 20 × microscope objective. The fibre samples ranging from 20cm to about 60cm in length were used in experiments. The experimental setup used was as shown in fig (3.1). The experimental procedure was as described in section 3.2.1.

3.2.3 Quantronix 114 at 1.06 μm

A Q-switched Quantronix 114 Nd: YAG laser was used to carry out experiments at 1.06 μm. The Q- Switch envelope width was 220 ns with a rate 2 kHz. A 20X microscope objective lens was used to launch radiations into the fibre. A KTP crystal was used to produce second harmonic green light at 532 nm which along with infrared from laser was launched into the fibre sample using a 20 X microscope objective. The fibre samples of

more than 1.5 km in length were used in experiments. The experimental setup used was as shown in fig (3.1). The experimental procedure was as described in section 3.2.1.

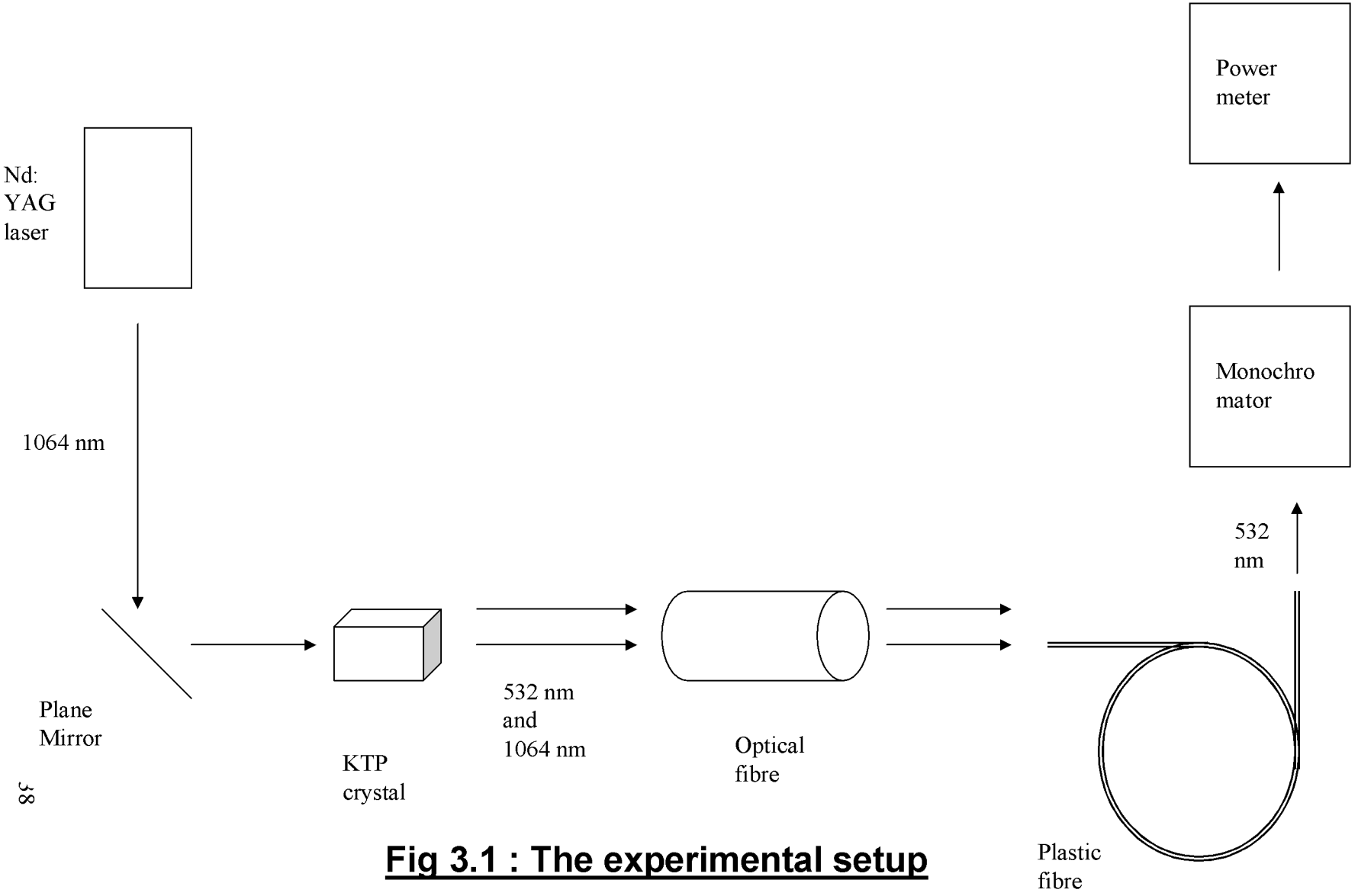

Fig 3.1 : The experimental setup

3.3 SHG and Other Upconversion Observations

3.3.1 Conditioning of Optical fibre

The fundamental infrared and the externally generated green by KTP crystal were launched into the optical fibre sample, monitoring the fibre output power using a power meter. After some time, about 15 min (slightly different for different fibre types), the power meter reading started going higher as a result of frequency doubling taking place inside optical fibre sample. Exposing the optical fibre samples to frequency doubled radiations along with fundamental radiations reduces its frequency doubling time from several hours to few minutes. The output was monitored from time to time while blocking the externally generated green radiations. The seed green light was blocked using the sharp cut filter at different time intervals before entering the optical fibre, in order to look at the frequency doubled radiations produced only by the optical fibre. After sometime the second harmonic radiations from the optical fibre were developed and they were visible. Second harmonic generated green light by optical fibre was observed using a power meter from time to time while filtering out any infrared radiations present in the optical fibre output using the plastic optical fibre. The plastic fibre has a high loss rate for infrared radiations so nearly all the infrared radiation is lost after passing through a few meters of plastic fibre and the only radiations that reach the power meter detector are the frequency doubled green radiations. The SH green grows with time from its initial value and reaches a maximum value.

3.3.2 The Output measurement

The output from the optical fibre was measured using a power meter. The output from the optical fibre was observed more deeply using a mono-chromator. Using mono-chromator

the power can be observed at different wavelengths. An electric motor was attached to gradually tune monochromator to different wavelengths. The output from the monochromator was connected to power meter to get the power measured at different wavelengths. The power at different wavelengths could be plotted against time using an xt plotter which was connected to power meter. Both infrared and the green light from KTP crystal were launched into the fibre sample. Seed green was blocked using the cut-off filter at different time intervals and output from the fibre sample was observed with time.

3.3.3 The Output

Along with second harmonic green light peak at 532nm some other high power peaks were also observed in the spectrums produced using xt plotter, which indicated the presence of other wavelengths in the optical fibre output. That compels us to the idea that there are some other processes happening inside optical fibre along with second harmonic process.

Along with second harmonic green light peak at 532nm some other peaks at frequencies as 355nm, 585nm, 660nm, 709nm and 820 nm were also observed in spectrums from fibre samples as can be seen in figures (3.2,3.3, 3.4, 3.5, 3.6, 3.7, 3.8, 3.9, 3.10, 3.11 and 3.12).

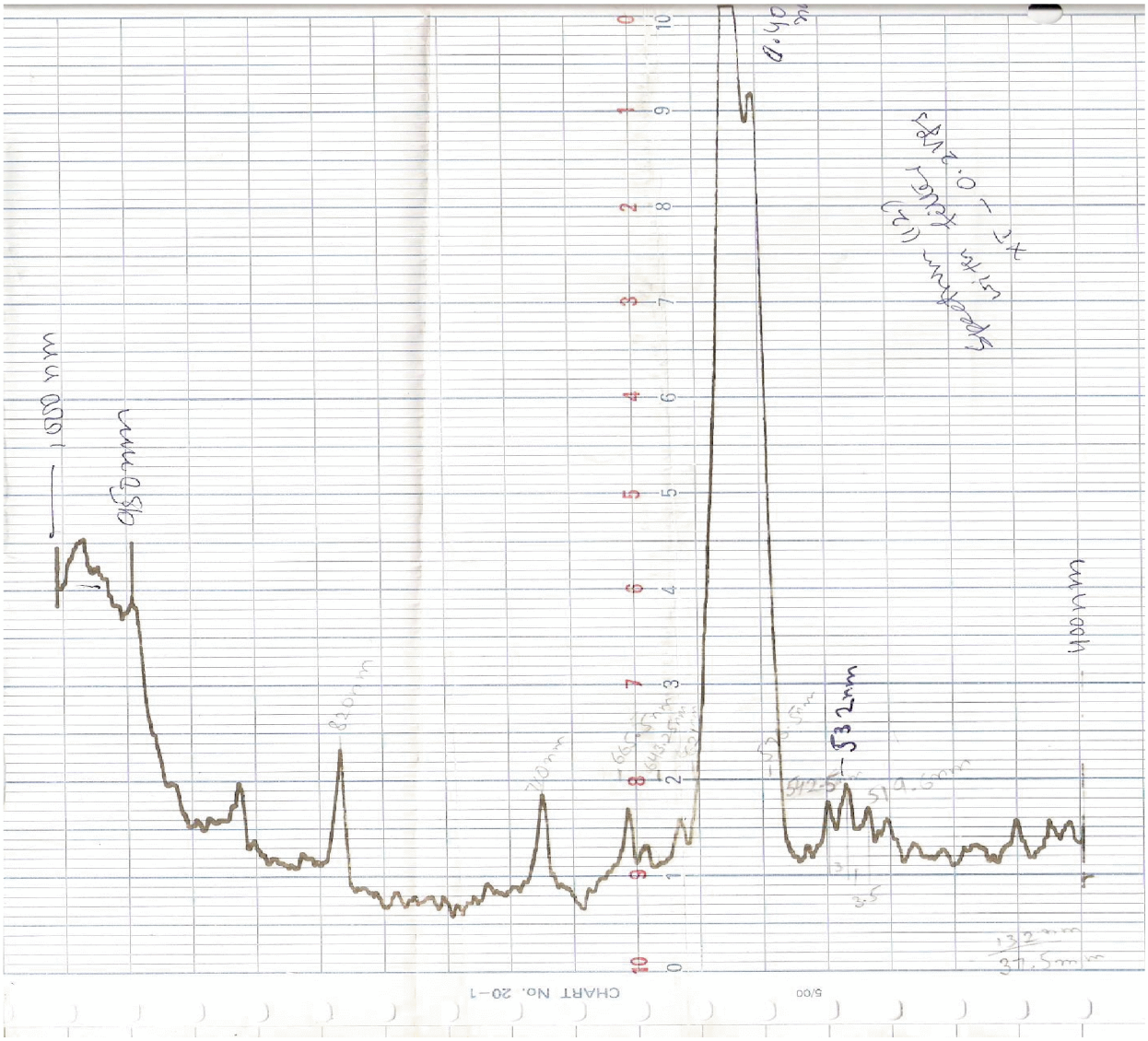

Fig (3.2): The high germanium optical fibre spectrum for the range 400nm to 1000nm for 1.06 µm pump radiation

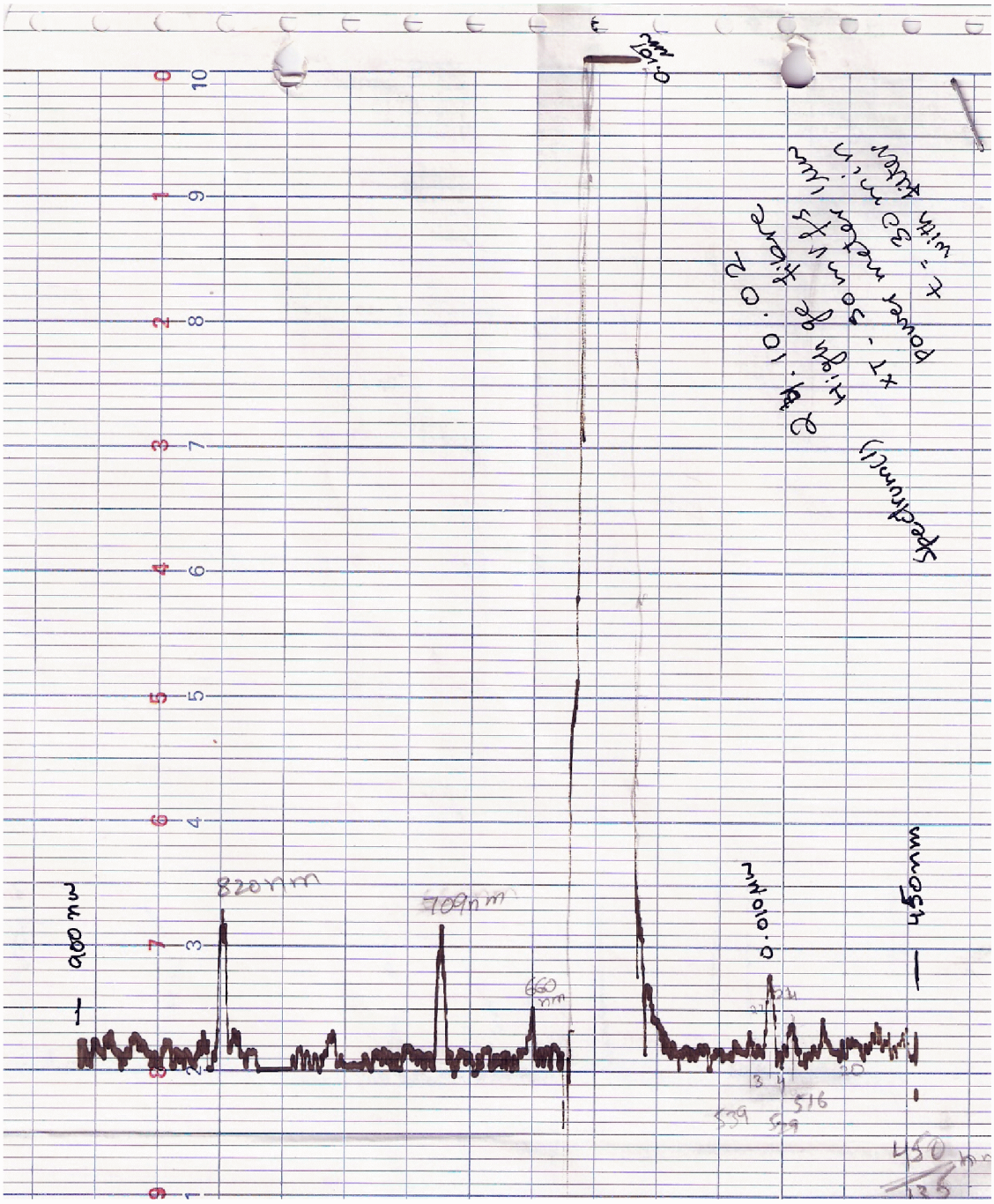

Fig (3.3): The high germanium optical fibre spectrum for the range 450nm to 900nm for 1.06 µm pump radiation

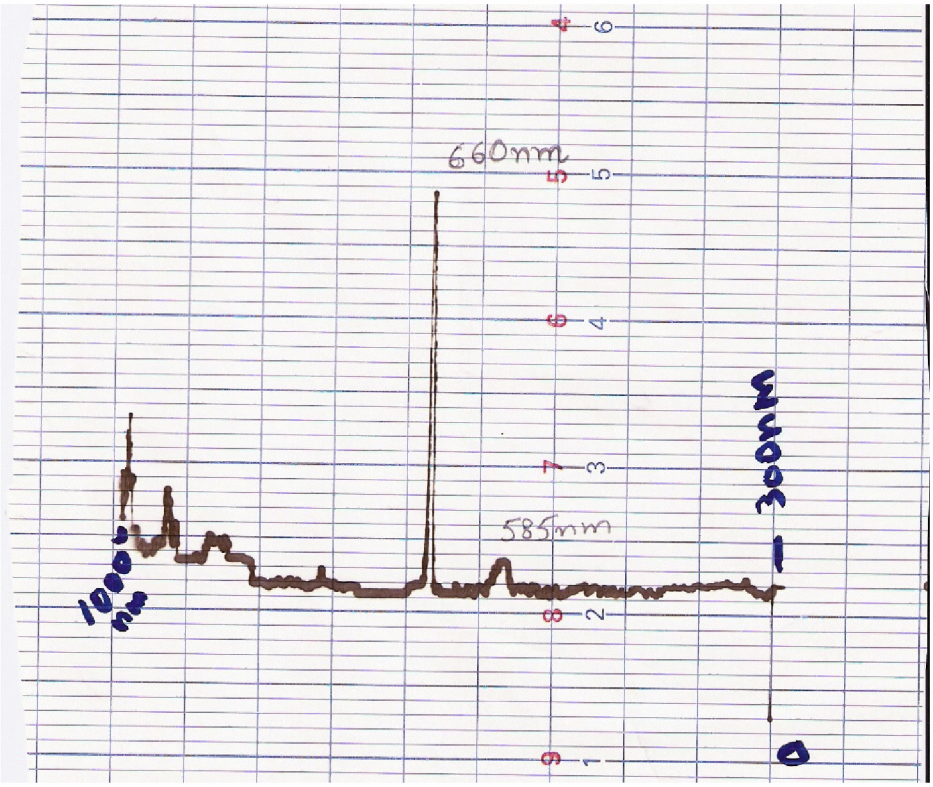

Fig (3.4): The high germanium optical fibre spectrum for the range 300nm to 1000nm for 1.319 µm

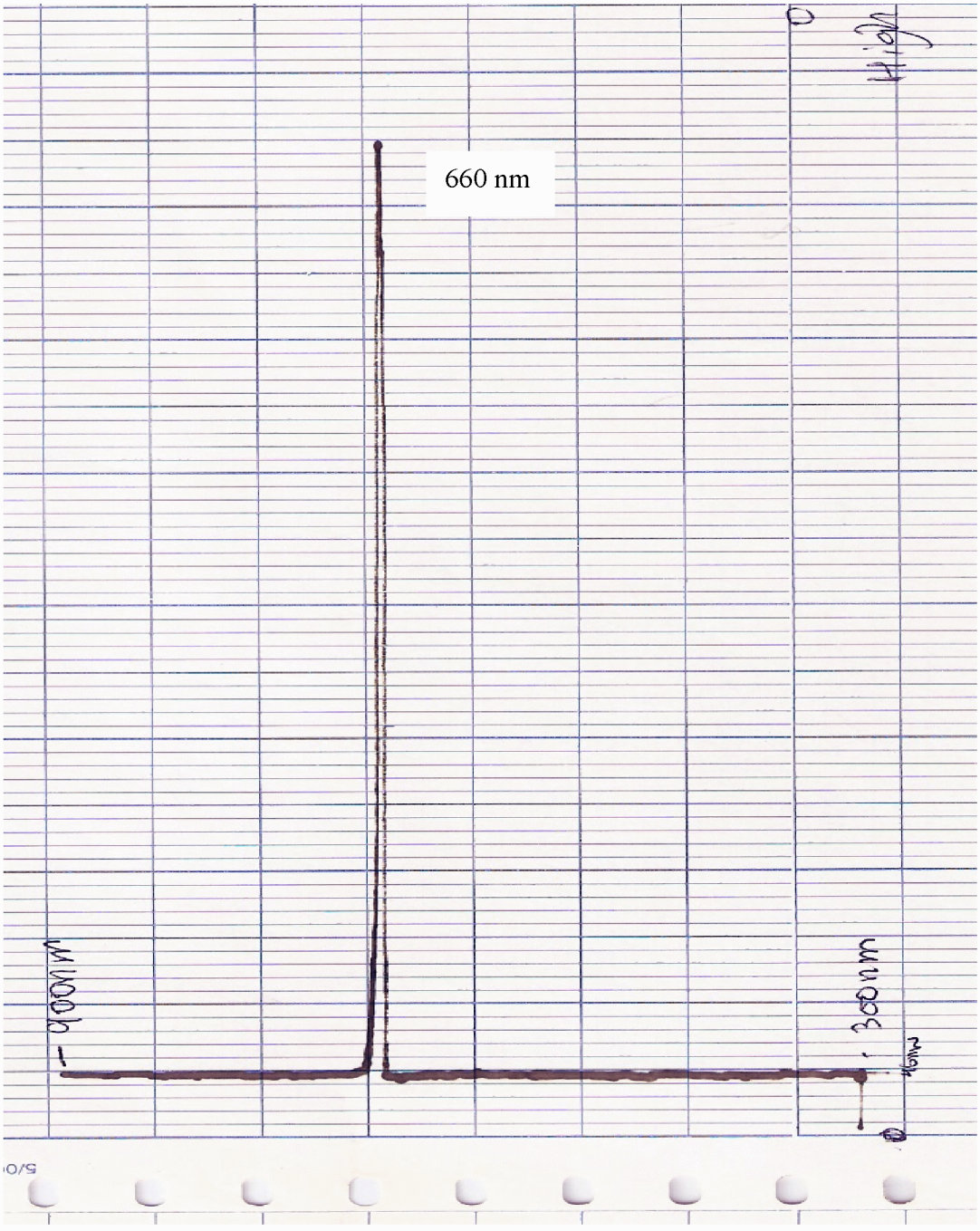

Fig (3.5): The high germanium optical fibre spectrum for the range 300nm to 900nm for 1.319 µm

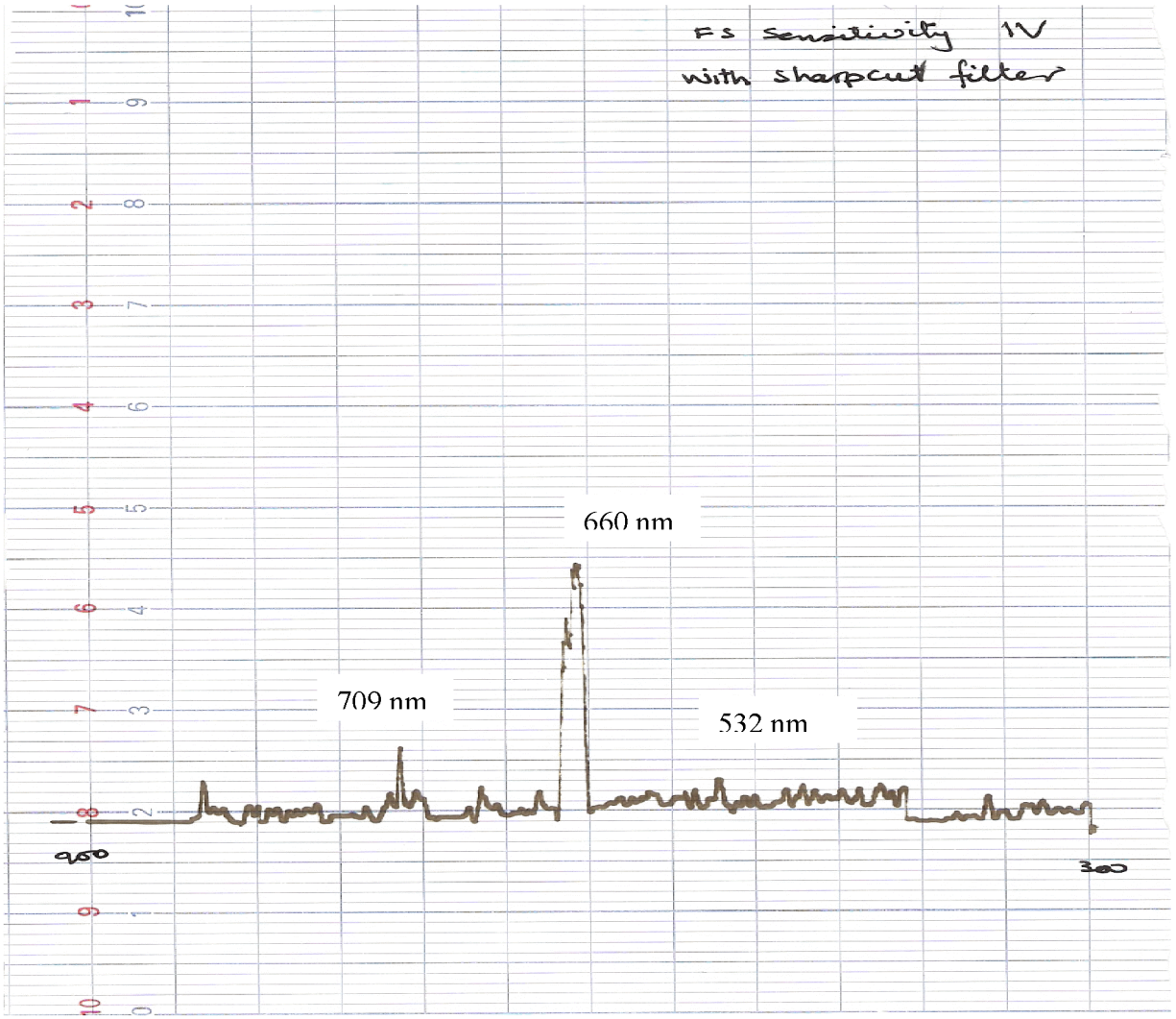

Fig (3.6): The > 1.5 km fibre sample spectrum for the range 300nm to 900nm for 1.06 µm pump radiation

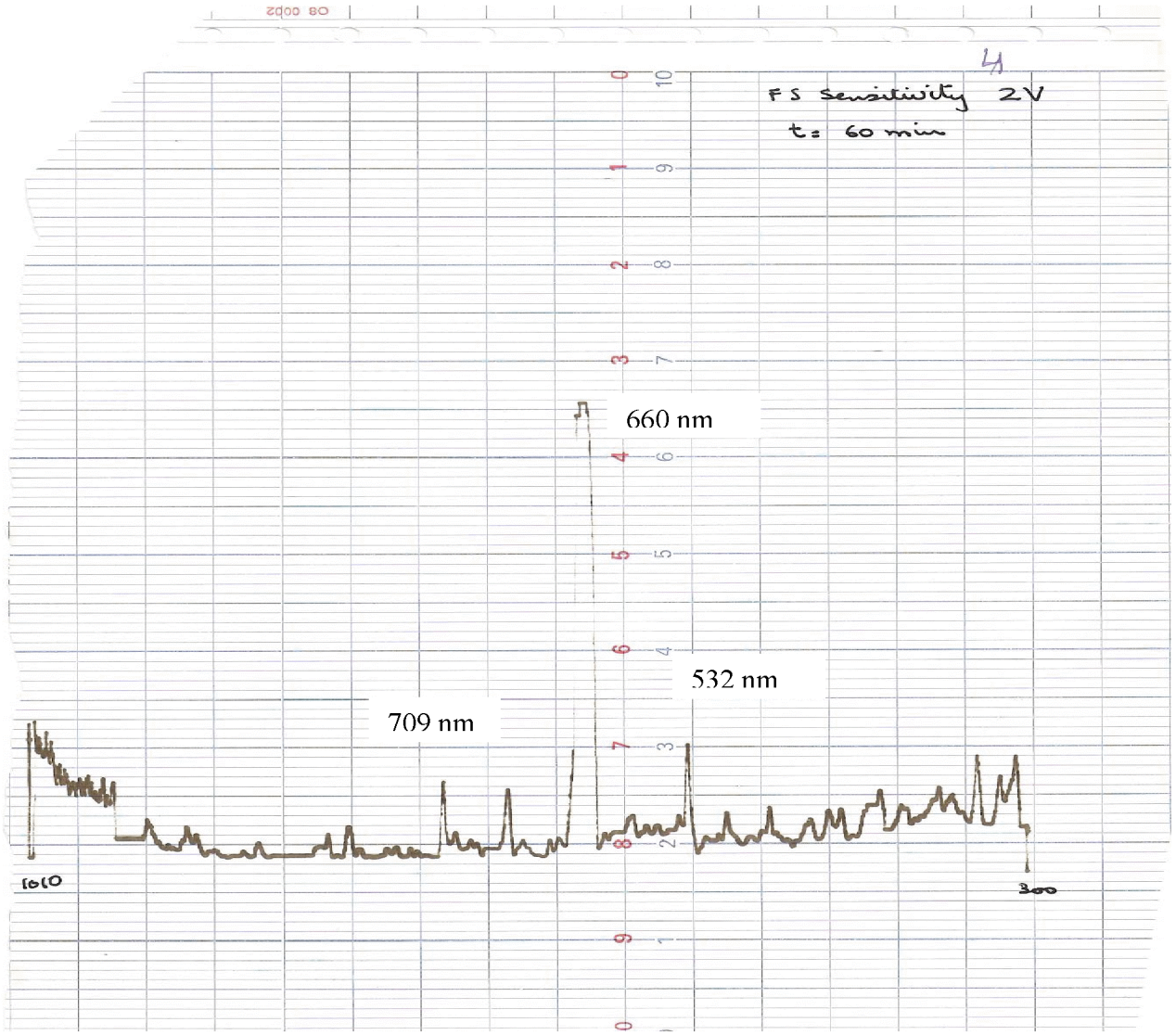

Fig (3.7): The > 1.5 km fibre sample spectrum for the range 300nm to 1050nm for 1.06 µm pump radiation

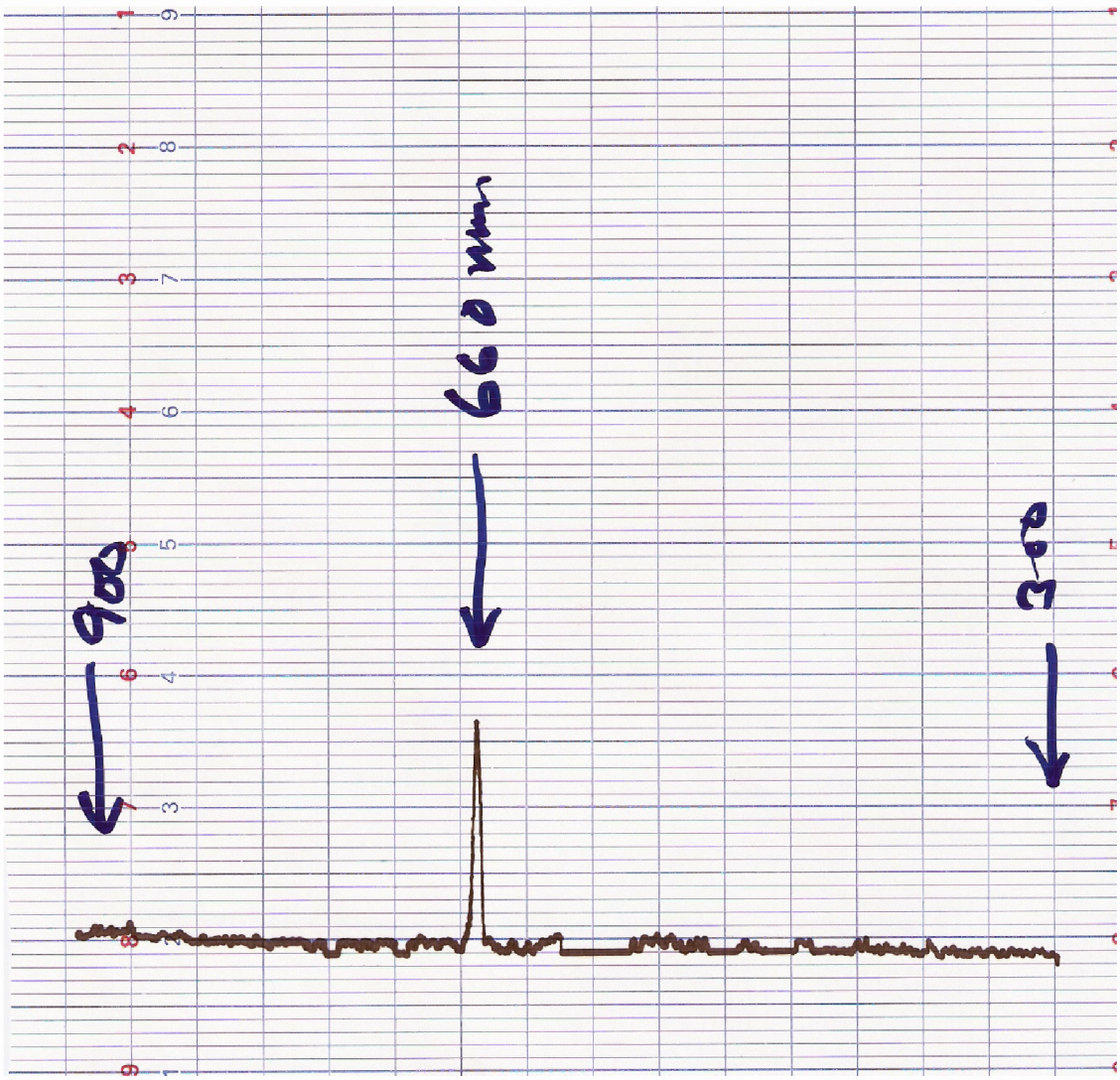

Fig (3.8): The > 1.5 km fibre sample spectrum for the range 300nm to 900nm for 1.319 µm pump radiation

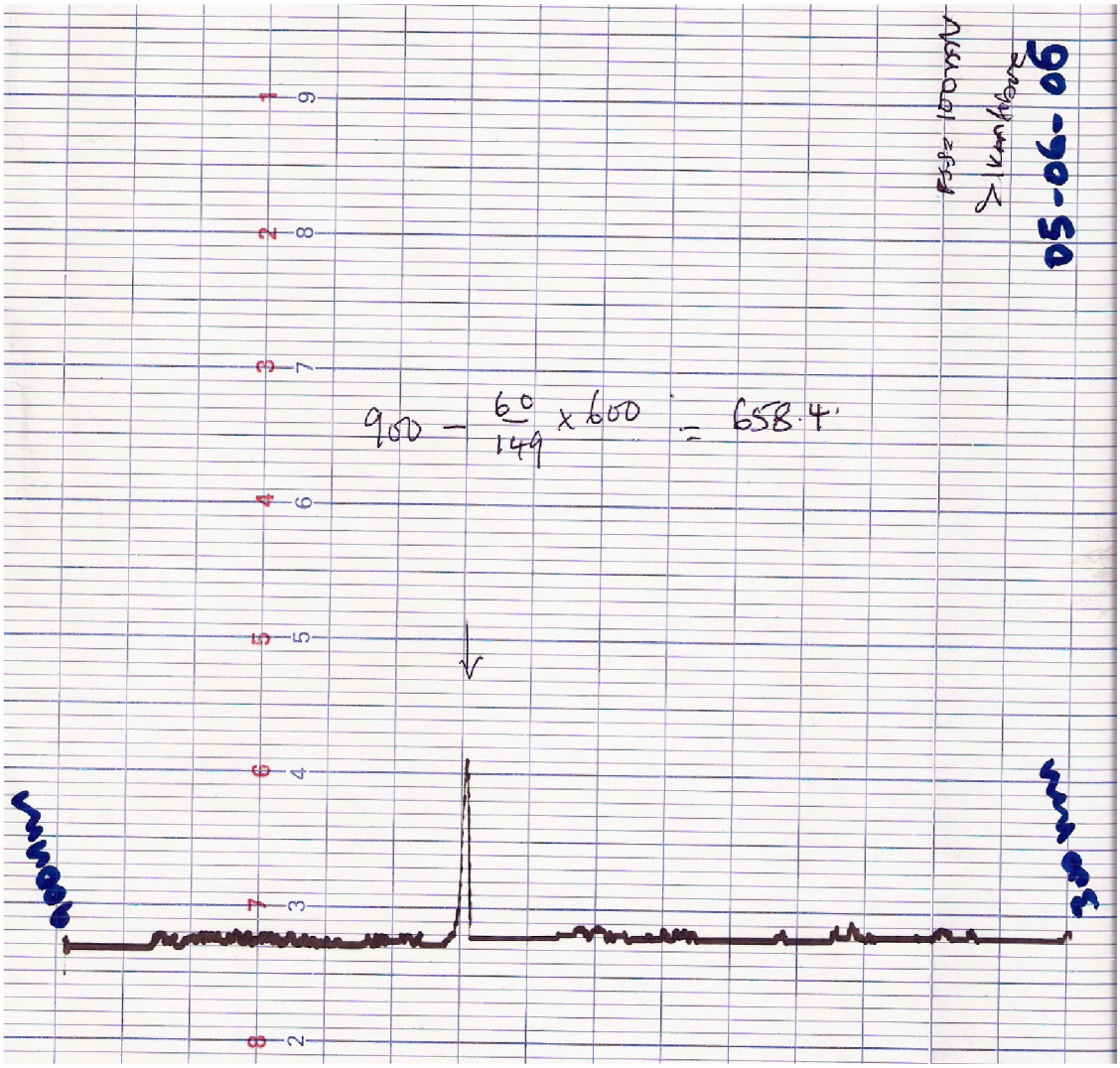

Fig (3.9): The > 1.5 km fibre sample spectrum for the range 300nm to 900nm for 1.319 µm pump radiation

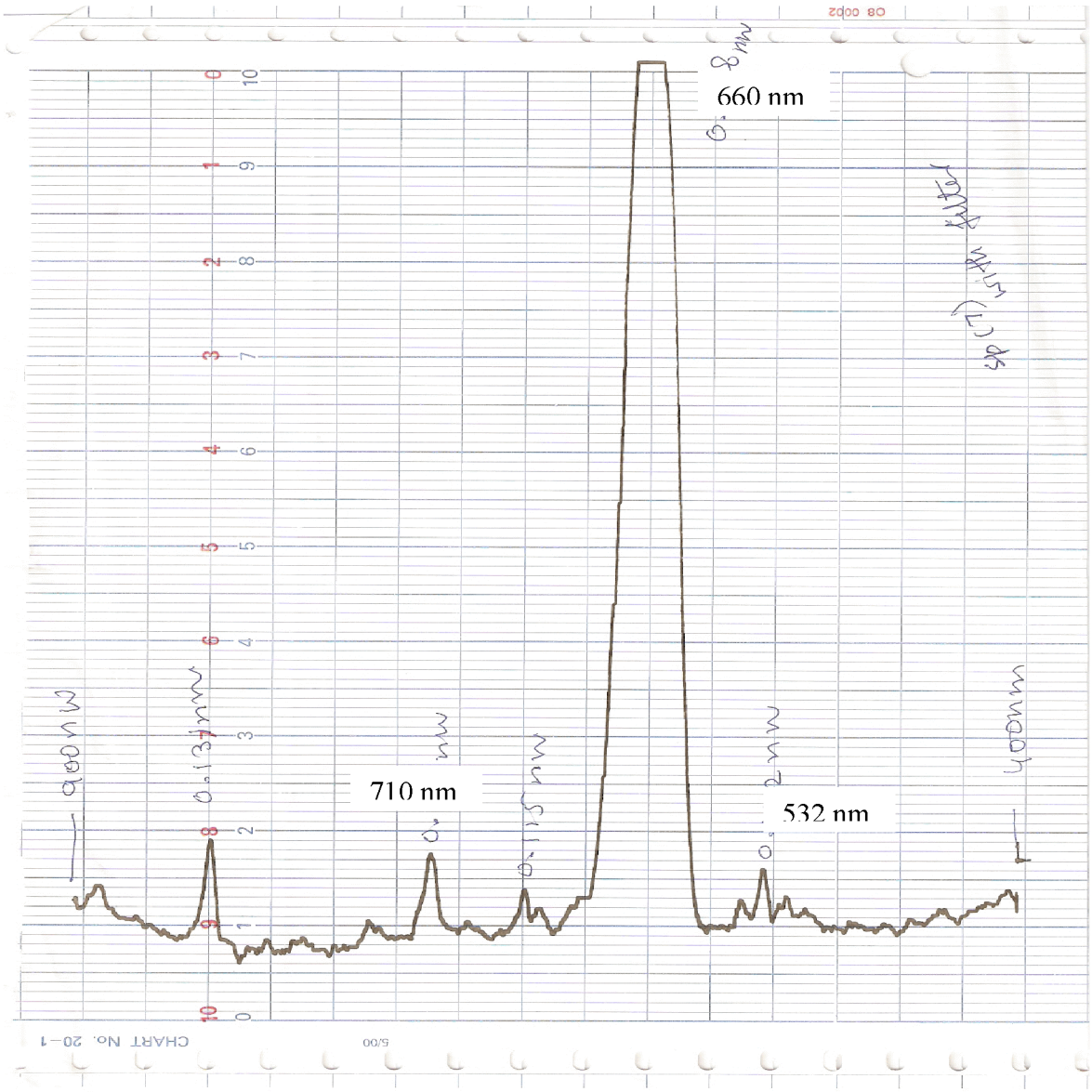

Fig (3.10): The optical fibre spectrum for the range 400nm to 900nm for 1.06 µm pump radiation

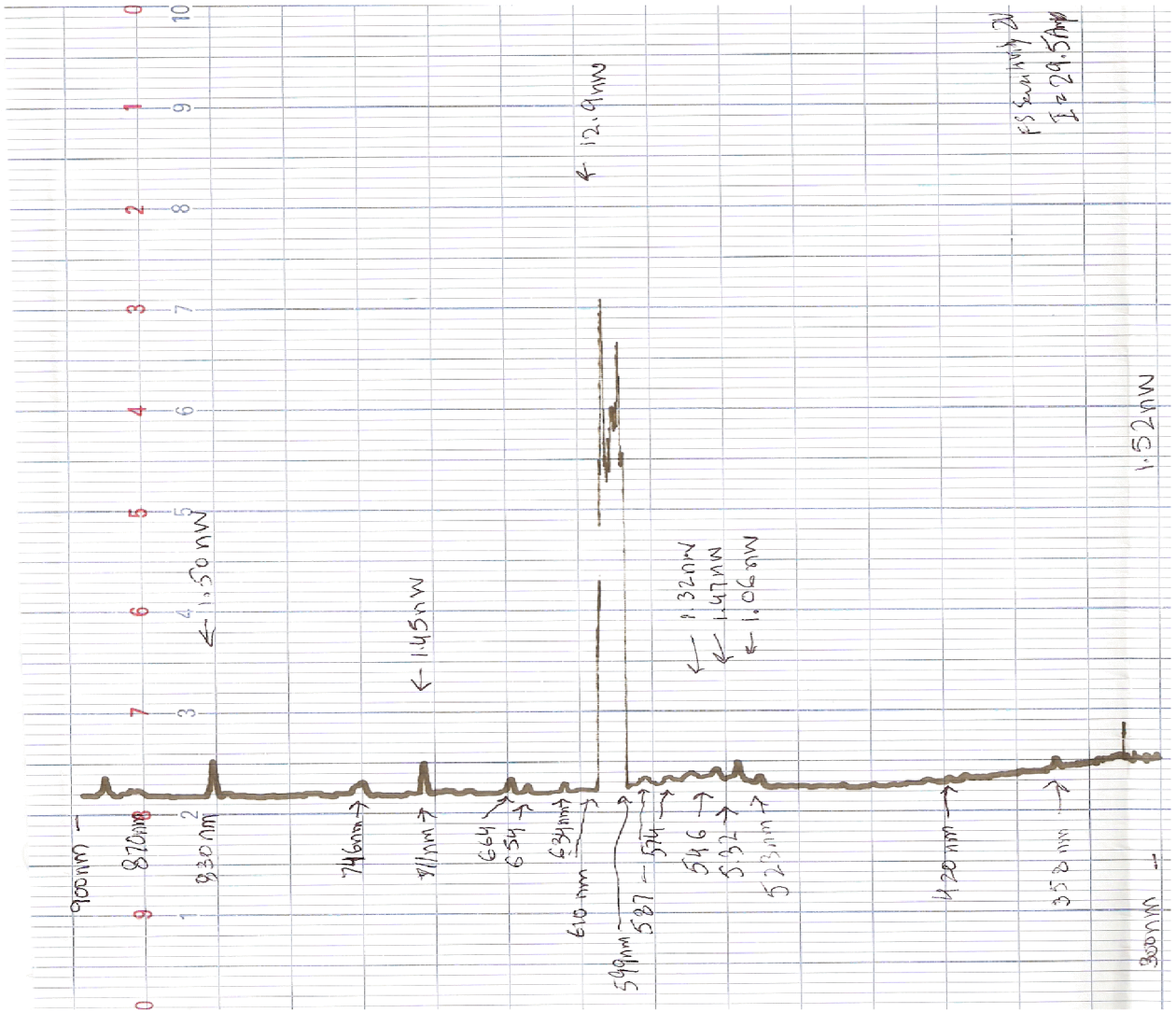

Fig (3.11): The fibre core optical fibre spectrum for the range 300nm to 900nm for 1.06 µm pump radiation

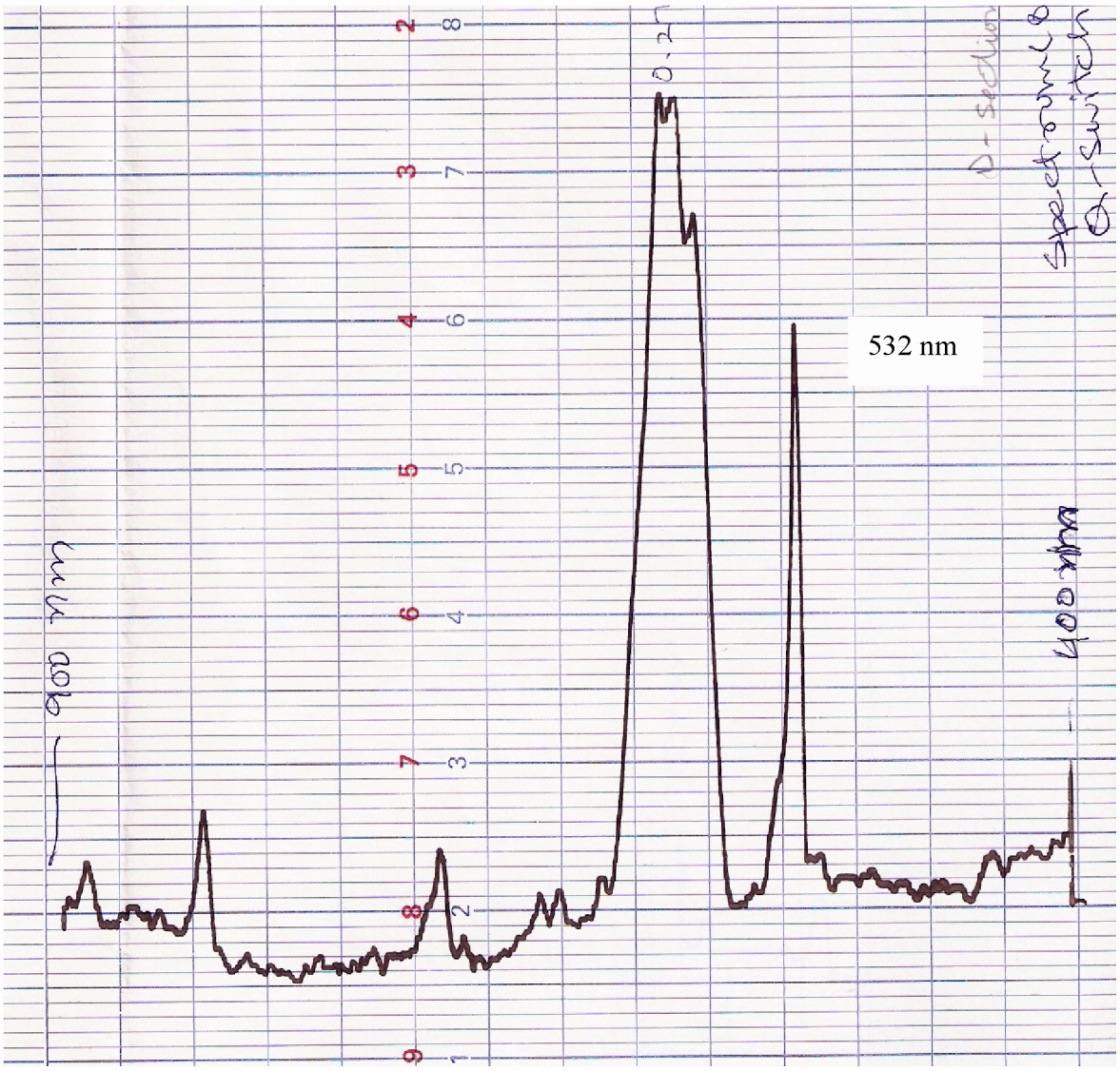

Fig (3.12): The D-section optical fibre spectrum for the range 400nm to 900nm for 1.06 µm pump radiation

References:

1. A. Yariv; Optical electronics in modern communications, fifth edition, Oxford Uni press, 1997.
2. P. N. Butcher and D. Cotter; The elements of nonlinear optics; Cambridge university press, 1990.
3. A. H. Cherin; An introduction to optical fibres, McGraw-Hill International Editions, 1993.
4. A. S. L. Gomes, U. Österberg, J. R. Taylor; Spectral and Temporal Investigations of Nonlinearities in a Non-Polarization preserving Single-mode Optical Fibre, Appl. Phys. B 41, 235-240, 1986.
5. T. A. Nguty and R. J. Potton; Photochemical changes in hydrogen-loaded optical fibres with application to bragg grating formation, Meas. Sci. Technol, 8, 1055-1057, 1997.
6. A. V. Amosov and G. T. Petrovskii; oxygen-vacancy defects in quartz glasses, Sov. Phys. Dokl., 28, 24-25, 1983.
7. E. J. Friebele, D. L. Griscom, and G. H. Sigel; Defect centres in a germanium-doped silica-core optical fibre, J. Appl. Phys., 45, 3424-3428, 1974.
8. D. L. Griscom, E. J. Friebele and K. J. Long; Fundamental defect centres in glass: Electron spin resonance and optical absorption studies of irradiated phosphorus-doped silica glass and optical fibres, J. Appl. Phys., 54, 3743-3762, 1983.
9. P. Kaiser; Drawing-induced colouration in vitreous silica fibres, JOSA, 64, 475-481, 1974.
10. E. P. O'Reilly and J. Robertson; Theory of defects in vitreous silicon dioxide, Phys. Rev. B, 27, 3780-3795, 1983.
11. B. Batdorf, C. Krautschik, U. Osterberg, G. Stegeman, J. W. Leitch, J. R. Rotge and T. F. Morse, Study of the length dependence of frequency-doubled light in optical fibres, Optics Communications, 73, 393-397, 1989.
12. F. Ouellete, D. Gagnon and M. Poirer; Permanent photoinduced birefringence in a Ge-doped fibre, Appl. Phys. Lett., 58, 1813-1815, 1991.

13. D. Z. Anderson, V. Mizrahi and J. E. Sipe; Model for second harmonic generation in glass optical fibres based on asymmetric photoelectron emission from defect sites, Optics Letters, 16, 796-798, 1991.
14. D. M. Krol and J. R. Simpson; Photoinduced second-harmonic generation in rare-earth-doped aluminosilicate optical fibres, Optics Letters, 16, 1650-1652, 1991.
15. D. M. Krol, B. Ehrlich, R. H. Stolen and H. W. K. Tom; Experimental study of second-harmonic-generation saturation in fibres by phase modulation between the fundamental and second-harmonic writing beams, Optics Letters, 17, 396-398, 1992.
16. P. G. Kazansky, L. Dong and P. St. J. Russell; High second-harmonic nonlinearities in poles silicate fibres, University of Southampton, 1994.
17. W. Margulis, F. Laurell and B. Lesche; Imaging the nonlinear grating in frequency-doubling fibres, Letters to Nature, 378, 699-701, 1995.
18. P. K. Bachmann, D. U. Wiechert and T. P. Meeuwsen; Thermal expansion coefficient of doped and undoped silica prepared by means of PCVD, Journal of Material Science, 23, 2584-2588, 1988.
19. Q. Chen and W. P. Risk; High efficiency quasi-phasematched frequency doubling waveguides in $KTiOPO_4$ fabricated by electric poling, Optics Letters, 32, 107-108, 1996.
20. A. Kiryanov, V. Aboites and I. V. Melnikov; Enhancing type-II optical second-harmonic generation by use of a laser beam with a rotating azimuth of polarization. Applied Physics Letters, 78, 874-876, 2001.

Chapter 4

Diffusion of hydrogen in silica

4.1 SHG in different optical fibres

Second harmonic generation has been observed in different types of optical fibres. Their characteristics and features are described later in this chapter. All of these fibres showed second harmonic generation with different efficiencies and different seeding times varying from 15 min to 30 min depending on seeding conditions particularly the power coupled into the fibre sample. High germanium fibre gave highest value for second harmonic produced.

The optical fibre type used by Gomes *et. al.* was the non-polarization preserving fibre, single-mode at 1.06 μm. They used optical fibre samples of lengths 1.5m and 120m. Margulis *et. al.* used the phosphor-doped glass fibres as long as >100m and as short as <50cm. They used a cw mode-locked and Q-switched Quantronix 114 Nd: YAG laser at

1.06 μm. Peak conversion efficiency of more than 5% was achieved. Besides the second harmonic line at 0.53μm 15 other peaks were observed. The frequency doubling of 647.1nm was reported by Valk using Kr + laser in a single mode fibre with a purely Ge-doped core. Optical fibre with a phosphorus free core doped with only germanium exposed to high pressure hydrogen gas for several hours and heated in air at high temperature about 2500C-5000C for 8-24 hours showed an enhancement in second harmonic conversion efficiency after seeding with 1.06 μm and 532 nm light.

Different types of the optical fibres have been used so far as described before. All of these fibres used were single mode and circular in shape except for the type 4 that has a D-shaped cladding as shown in figure (4.1, 4.2, 4.3, 4.4, 4.5, 4.6, 4.7 and 4.8). The D-section fibre also shows some distinguished properties which are described in section 4.2.

The basic reason to use the D-section fibre was to reduce the hydrogen diffusion time into the optical fibre core. It takes about 1 week to diffuse hydrogen through the cladding of a normal circular fibre where as by using D- section fibre hydrogen can be diffused into the core in less than an hour. The spectrum of power versus time is shown in fig (3.12).

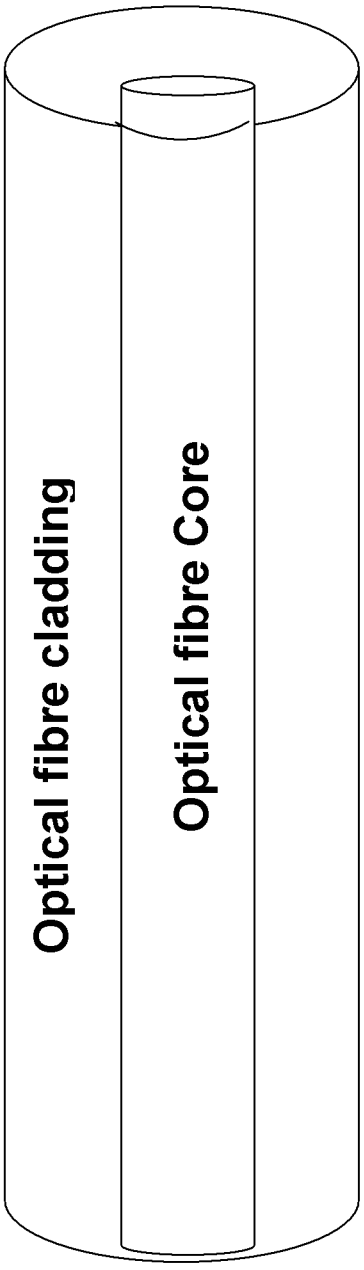

Fig 4.1 : The Optical fibre

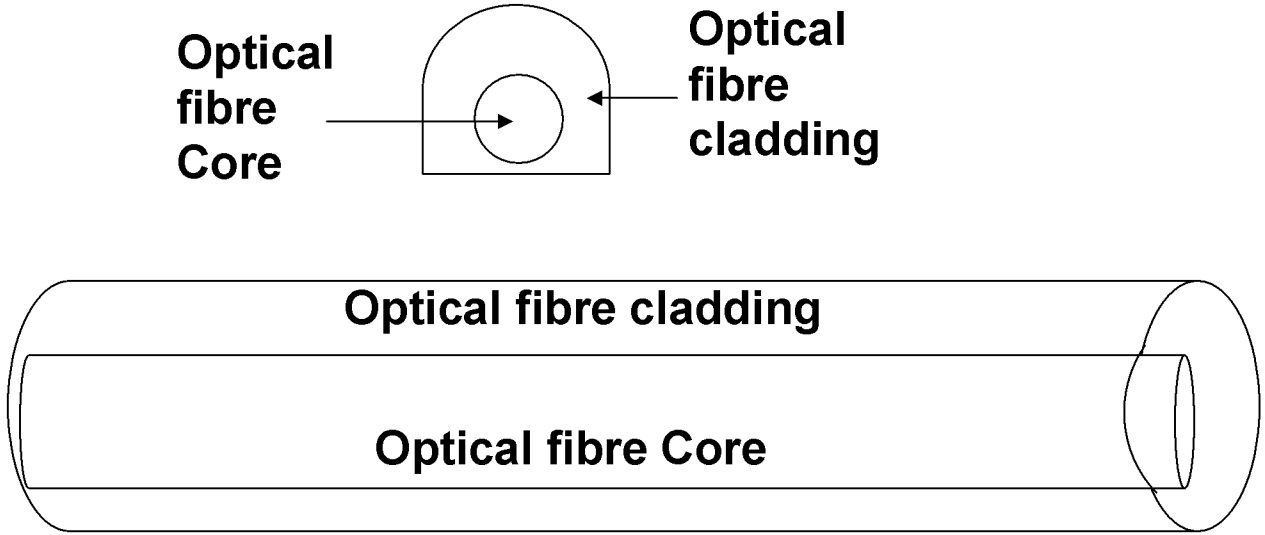

Fig 4.2 : The D-section Optical fibre

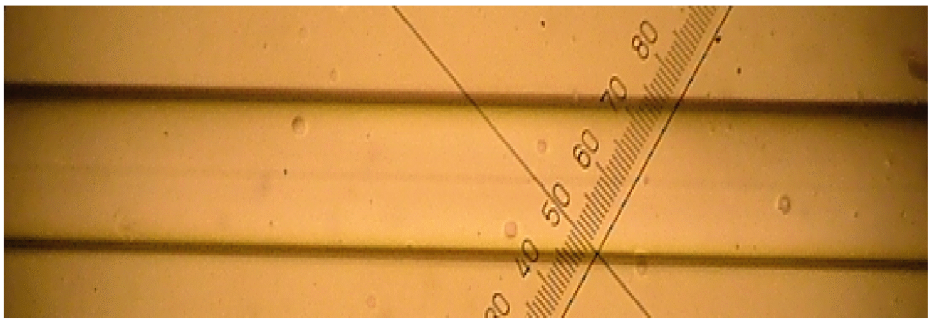

Fig (4.3): The Fibre core optical fibre sample observed using a phase contrast microscope

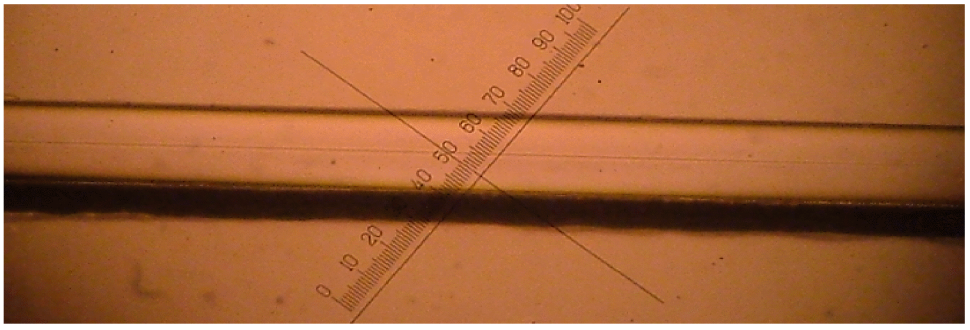

Fig (4.4): The high germanium optical fibre sample observed using a phase contrast microscope

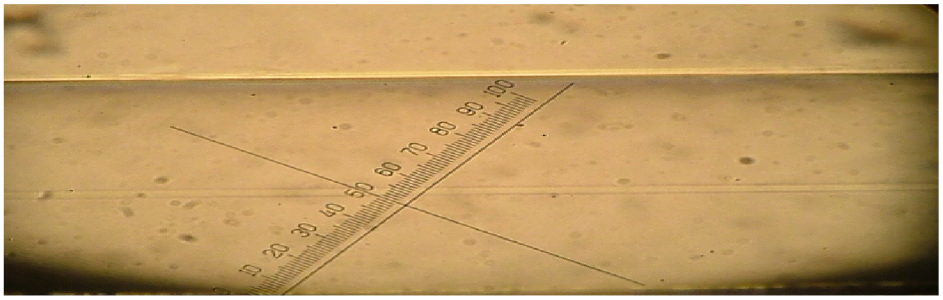

Fig (4.5): The optical fibre sample from optical fibre company observed using a phase contrast microscope

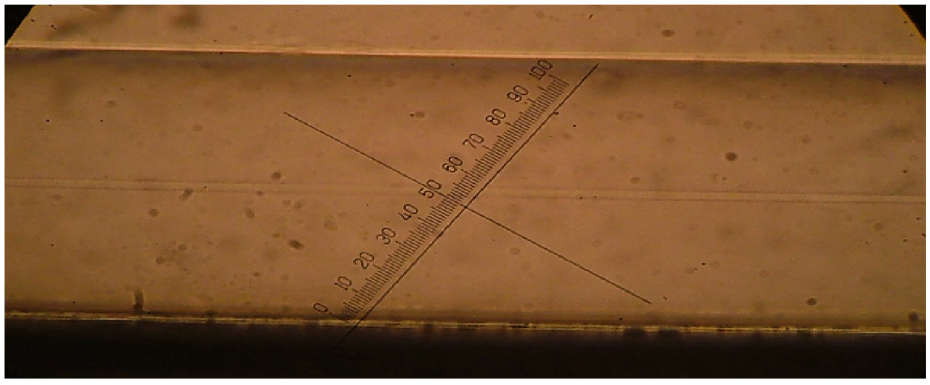

Fig (4.6): The long length optical fibre sample observed using a phase contrast microscope

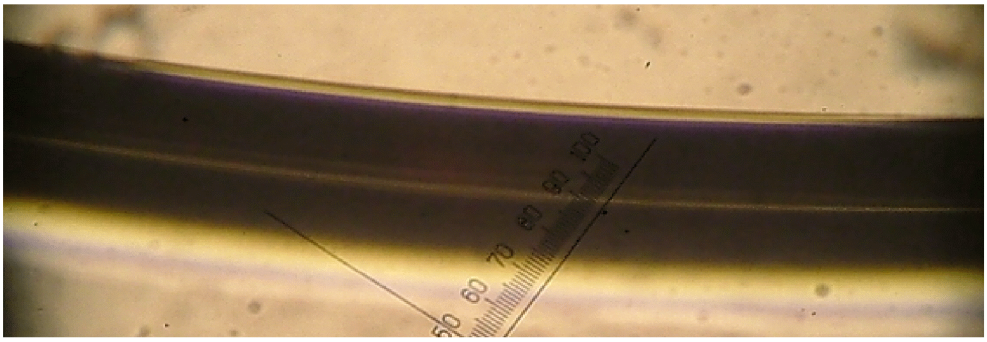

Fig (4.7): The D-section optical fibre sample observed using a phase contrast microscope

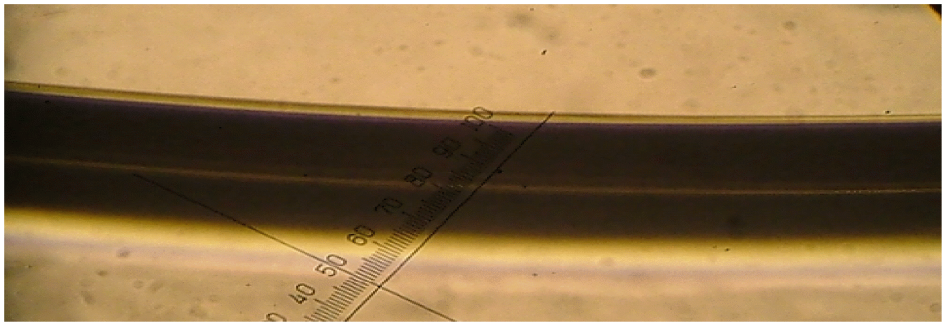

Fig (4.8): The D-section optical fibre sample observed using a phase contrast microscope

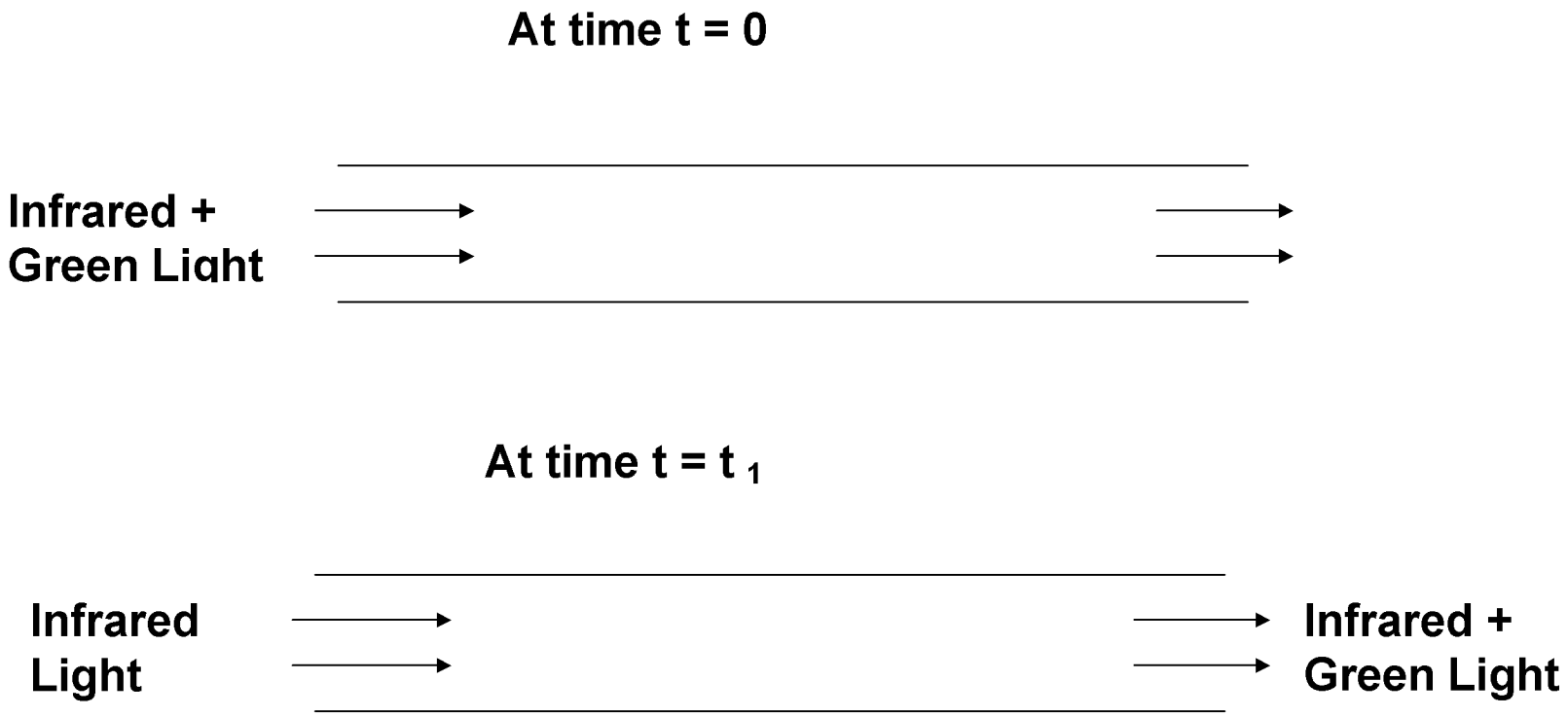

Fig 4.9 : Second harmonic generation in Optical fibre

4.2 Distinguishing features of D-Section optical fibre

The D-section optical fibre has an unsymmetrical cladding with the core closer to the flat surface, to get easier access to the guided field in cladding as shown in fig (4.7 and 4.8). However the reduced cladding thickness on one side of the fibre core changes the light guiding properties significantly. The major influence of reduced cladding is that in some circumstances a D-section fibre may not even support one guided mode and it is possible for even fundamental mode to cut-off at certain wavelength, this is analogue to infinite quantum well in quantum mechanics. The D-section fibre has some distinguishing properties from other normal optical fibres It has strong waveguide dispersion and scattered modes. It curves up on removing the coating and is non-symmetric in structure. SHG was observed when fibre was exposed to infrared with its coating removed.

The light guided through the D-section fibre was observed to be in higher mode i.e. LP_{31} mode. On rotating the fibre the mode pattern was observed to change to a different pattern. On rotating output end of the fibre through 45^{o} mode pattern changes to a lower order. On further rotating by 45^{o} LP_{31} mode reappears. On further rotation it shows LP_{21} mode. Also the power of light guided through the optical fibre changes with different mode patterns on rotation with higher power value with a lower order mode. The D-section fibre bends away from its flat surface as seen under phase contrast microscope.

When infrared light is seeded into the optical fibre and alignment adjusted to get highest power it goes down rapidly with time. It might be happening that some other wavelengths are produced in the fibre which are invisible but guided through the plastic fibre and power meter captures them. No infrared light was observed to be guided through the D-section fibre while using its sample with the coating not removed. The green light seemed to be getting through though as it could be detected by the power meter.

4.3 Hydrogen Diffusion into the Optical fibre

One of the methods used to enhance SHG is diffusion of hydrogen into the fibre and heating. Hydrogen is chosen because it is shown to react with defects present in glass at high temperature.

The apparatus used for hydrogen diffusion was same as used before only a capillary tube was added in the setup to hold the optical fibre samples inside it. Both ends of the tube were sealed using black wax to keep it filled with hydrogen gas. The capillary tubes were specifically designed as shown in figure (4.10) with two side arms to put the optical fibres inside them and to get hydrogen into and out of capillary tubes as needed. Polythene tubes were attached to the side arms of the capillary tube, used as inlet and outlet for hydrogen, to prevent any damage by movement of the tube while filling it with hydrogen. A hot air blower was used to melt the black wax and seal the both ends of capillary tube. Hydrogen gas was stored in balloons. One polythene tube used as input end was attached to a balloon with a clamp on its opening. This clamp was loosened as much needed to get hydrogen in the capillary tube. The other tube used as output end was closed with a clamp so it could be opened to let hydrogen out.

Hydrogen can be diffused in D-section fibre in very less time as compared to normal circular fibres. As with normal circular fibres it can take up to a week to diffuse hydrogen. The time for the diffusion of molecular hydrogen through the cladding of a circular single mode optical fibre is about 1 week. The effects of in-diffused hydrogen can be seen in less than 1 hour by using the reduced cladding thickness.

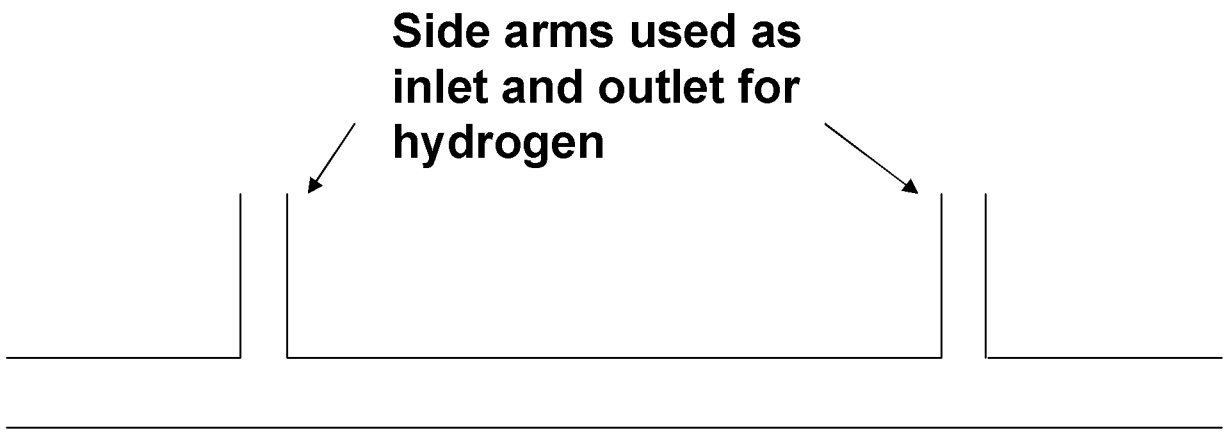

Fig 4.10 : The Capillary tube used for hydrogen diffusion

4.4 Monochromator Calibration

Monochromator was calibrated using a cadmium lamp and a mercury lamp. Radiations from these lamps were guided through the monochromator and spectrums were plotted using xt-plotter at different wavelengths ranging from 300 to 1000 nm.

4.4.1 Experimental setup

The cadmium lamp was mounted on a mount so that radiations from it enter the monochromator without much loss. The monochromator wavelength was changed continuously using an electric motor and the output power was measured. To measure output power from monochromator, its output was fed into a power-meter. The power meter was connected to a chart plotter which plotted the power measured by the power meter against time. The cadmium lamp was replaced with a mercury lamp to obtain a different set of spectral lines. The spectra obtained are shown in figures (4.13 – 4.14). The wavelengths for peak powers observed in the spectra were then compared with two references as given in figure (4.11) and (4.12). The tables to compare the wavelengths are given below. The wavelengths for high peaks were plotted against the reference wavelengths as shown in figure (4.17) and the gradient and intercept for best fit line were found out. It was found out that monochromator is calibrated well by a gradient value of 1.004 (+/-) 0.008 and an intercept of value -3.4 (+/-) 3.8.

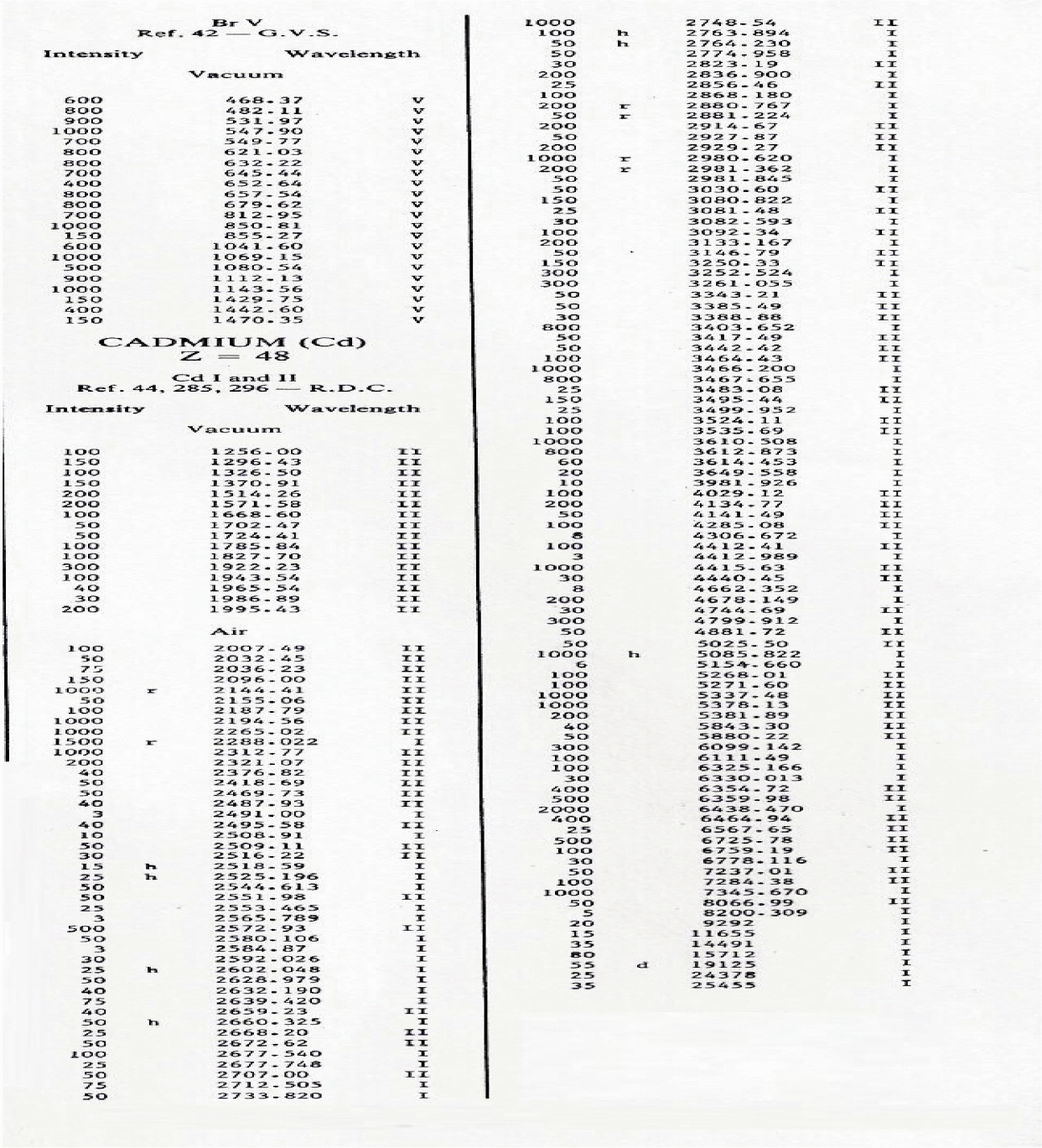

Br V
Ref. 42 — G.V.S.

Intensity		Wavelength	
		Vacuum	
600		468.37	V
800		482.11	V
900		531.97	V
1000		547.90	V
700		549.77	V
800		621.03	V
800		632.22	V
700		645.44	V
400		652.64	V
800		657.54	V
800		679.62	V
700		812.95	V
1000		850.81	V
150		855.27	V
600		1041.60	V
1000		1069.15	V
500		1080.54	V
900		1112.13	V
1000		1143.56	V
150		1429.75	V
400		1442.60	V
150		1470.35	V

CADMIUM (Cd)
Z = 48

Cd I and II
Ref. 44, 285, 296 — R.D.C.

Intensity		Wavelength	
		Vacuum	
100		1256.00	II
150		1296.43	II
100		1326.50	II
150		1370.91	II
200		1514.26	II
200		1571.58	II
100		1668.60	II
50		1702.47	II
50		1724.41	II
100		1785.84	II
100		1827.70	II
300		1922.23	II
100		1943.54	II
40		1965.54	II
30		1986.89	II
200		1995.43	II
		Air	
100		2007.49	II
50		2032.45	II
75		2036.23	II
150		2096.00	II
1000	r	2144.41	I
50		2155.06	II
100		2187.79	II
1000		2194.56	II
1000		2265.02	II
1500	r	2288.022	I
1000		2312.77	II
200		2321.07	II
40		2376.82	II
50		2418.69	II
50		2469.73	II
40		2487.93	II
3		2491.00	I
40		2495.58	II
10		2508.91	I
50		2509.11	II
30		2516.22	II
15	h	2518.59	I
25	h	2525.196	I
50		2544.613	I
50		2551.98	II
25		2553.465	I
3		2565.789	I
500		2572.93	II
50		2580.106	I
3		2584.87	I
30		2592.026	I
25	h	2602.048	I
50		2628.979	I
40		2632.190	I
75		2639.420	I
40		2659.23	II
50	h	2660.325	I
25		2668.20	II
50		2672.62	II
100		2677.540	I
25		2677.748	I
50		2707.00	II
75		2712.505	I
50		2733.820	I
1000		2748.54	II
100	h	2763.894	I
50	h	2764.230	I
50		2774.958	I
30		2823.19	II
200		2836.900	I
25		2856.46	II
100		2868.180	I
200	r	2880.767	I
50	r	2881.224	I
200		2914.67	II
50		2927.87	II
200		2929.27	II
1000	r	2980.620	I
200	r	2981.362	I
50		2981.845	I
50		3030.60	II
150		3080.822	I
25		3081.48	II
30		3082.593	I
100		3092.34	II
200		3133.167	I
50		3146.79	II
150		3250.33	II
300		3252.524	I
300		3261.055	I
50		3343.21	II
50		3385.49	II
30		3388.88	II
800		3403.652	I
50		3417.49	II
50		3442.42	II
100		3464.43	II
1000		3466.200	I
800		3467.655	I
25		3483.08	II
150		3495.44	II
25		3499.952	I
100		3524.11	II
100		3535.69	II
1000		3610.508	I
800		3612.873	I
60		3614.453	I
20		3649.558	I
10		3981.926	I
100		4029.12	II
200		4134.77	II
50		4141.49	II
100		4285.08	II
8		4306.672	I
100		4412.41	II
3		4412.989	I
1000		4415.63	II
30		4440.45	II
8		4662.352	I
200		4678.149	I
30		4744.69	II
300		4799.912	I
50		4881.72	II
50		5025.50	II
1000	h	5085.822	I
6		5154.660	I
100		5268.01	II
100		5271.60	II
1000		5337.48	II
1000		5378.13	II
200		5381.89	II
40		5843.30	II
50		5880.22	II
300		6099.142	I
100		6111.49	I
100		6325.166	I
30		6330.013	I
400		6354.72	II
500		6359.98	II
2000		6438.470	I
400		6464.94	II
25		6567.65	II
500		6725.78	II
100		6759.19	II
30		6778.116	I
50		7237.01	II
100		7284.38	II
1000		7345.670	I
50		8066.99	II
5		8200.309	I
20		9292	I
15		11655	I
35		14491	I
80		15712	I
55	d	19125	I
25		24378	II
35		25455	I

Fig (4.11): The reference used to compare cadmium spectrum

Page no.: 115.1
Issue no.: 3
Date: March 1974
Author: P A Young

WAVELENGTHS OF SPECTRAL LINES IN THE VISIBLE

(of some common elements in arc lamps)

R = Red; Y = Yellow; G = Green; BG = Blue-Green; B = Blue; V = Violet.

SODIUM

R 0.6161) 0.6154)	S
Y 0.5896) 0.5890)	P
G 0.5688) 0.5683)	D
G 0.5154) 0.5149)	S
BG 0.4983) 0.4979)	D
B 0.4669) 0.4665)	D
B 0.4498) 0.4494)	D

POTASSIUM

R 0.7699) 0.7665)	P
R 0.6939) 0.6911)	S
Y 0.5832) 0.5812)	D
Y 0.5802) 0.5782)	S
G 0.5359) 0.5343)	D
G 0.5340) 0.5323)	S

POTASSIUM

G 0.5112) 0.5097)	D
BG 0.5099) 0.5084)	S
BG 0.4965) 0.4950)	D
BG 0.4956) 0.4941)	S
B 0.4870) 0.4856)	D
V 0.4047) 0.4044)	P

S = Sharp; P = Principal; D = Diffuse.

MERCURY

Y0.5790	S
Y0.5770)	T
G0.5461)	T
BG0.4916	S
B0.4358	T
V0.4078	
V0.4047)	T

CADMIUM

R0.6439	S
G0.5086)	
BG0.4800)	T
B0.4678)	
V0.4415	

ZINC

R0.6362	S
G0.5182	S
BG0.4811)	
B0.4722)	T
B0.4680)	

S = Singlet; T = Triplet.

HYDROGEN

R0.6563	α
BG 0.4861	β
V0.4341	γ
V0.4102	δ

HELIUM

R0.7065	
R0.6678	S
Y0.5876	T
BG0.5047	S
BG0.5015	S
B0.4921	S
B0.4713	T
B0.4471	T
B0.4438	S
V0.4387	S
V0.4169	S

S = Singlet; T = Triplet

THALLIUM

G0.5350

All wavelengths in μm (microns) 1 μm = 10^{-6} metre.

Fig (4.12): The reference used to compare cadmium and mercury spectra

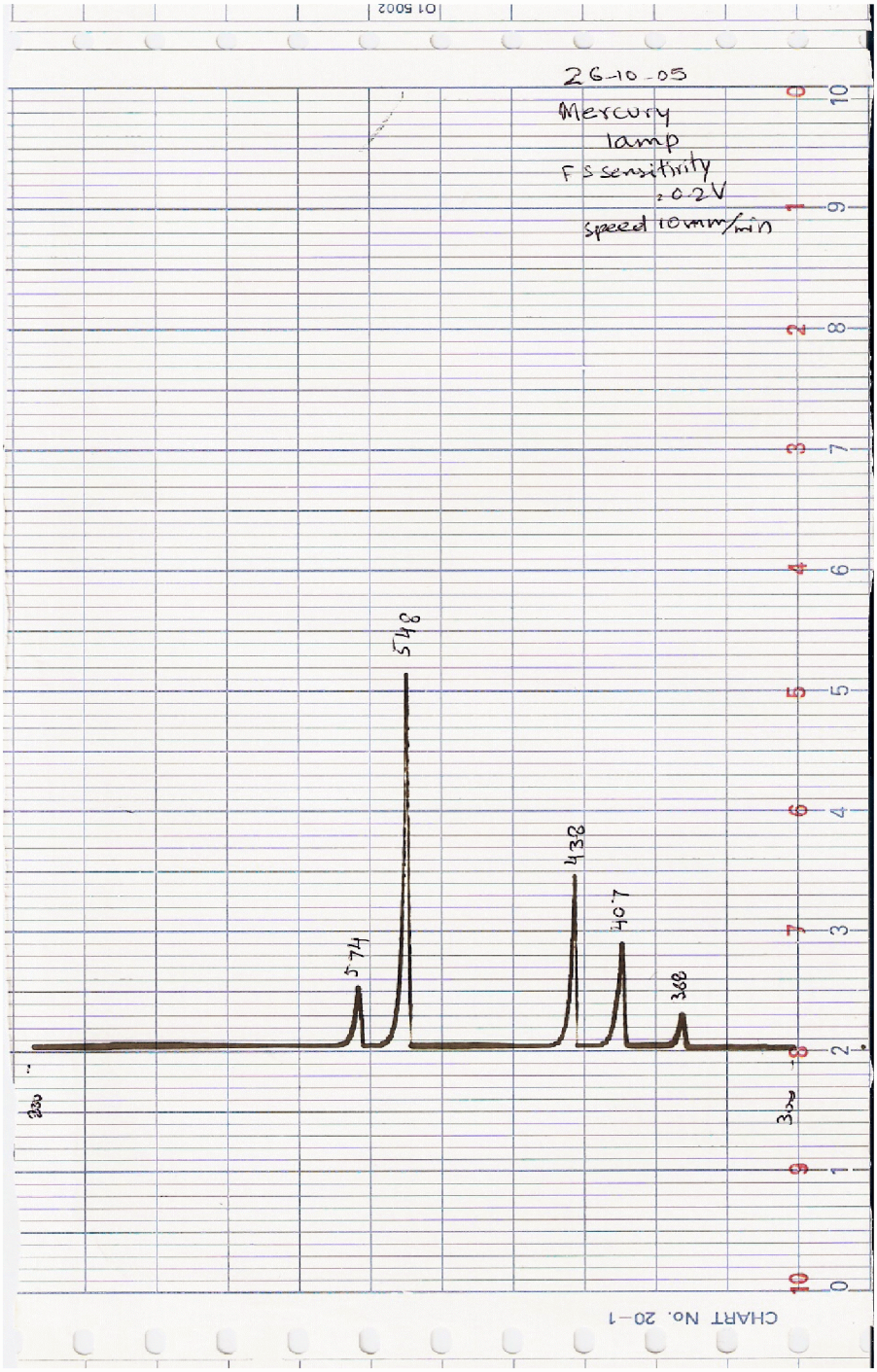

Fig (4.13): The mercury lamp spectrum for the wavelength range 300nm to 800nm

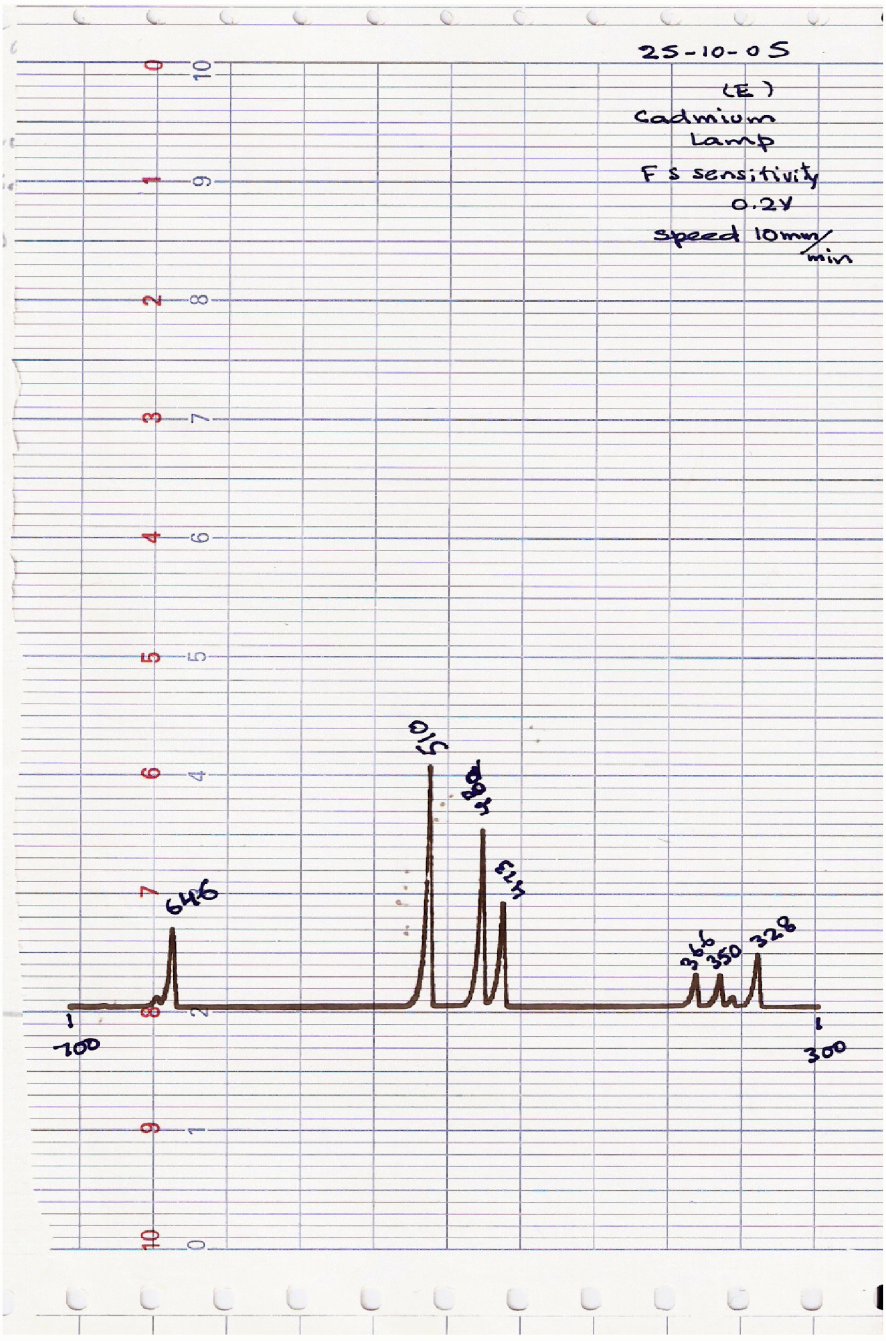

Fig (4.14): The cadmium lamp spectrum for the wavelength range 300nm to 700nm

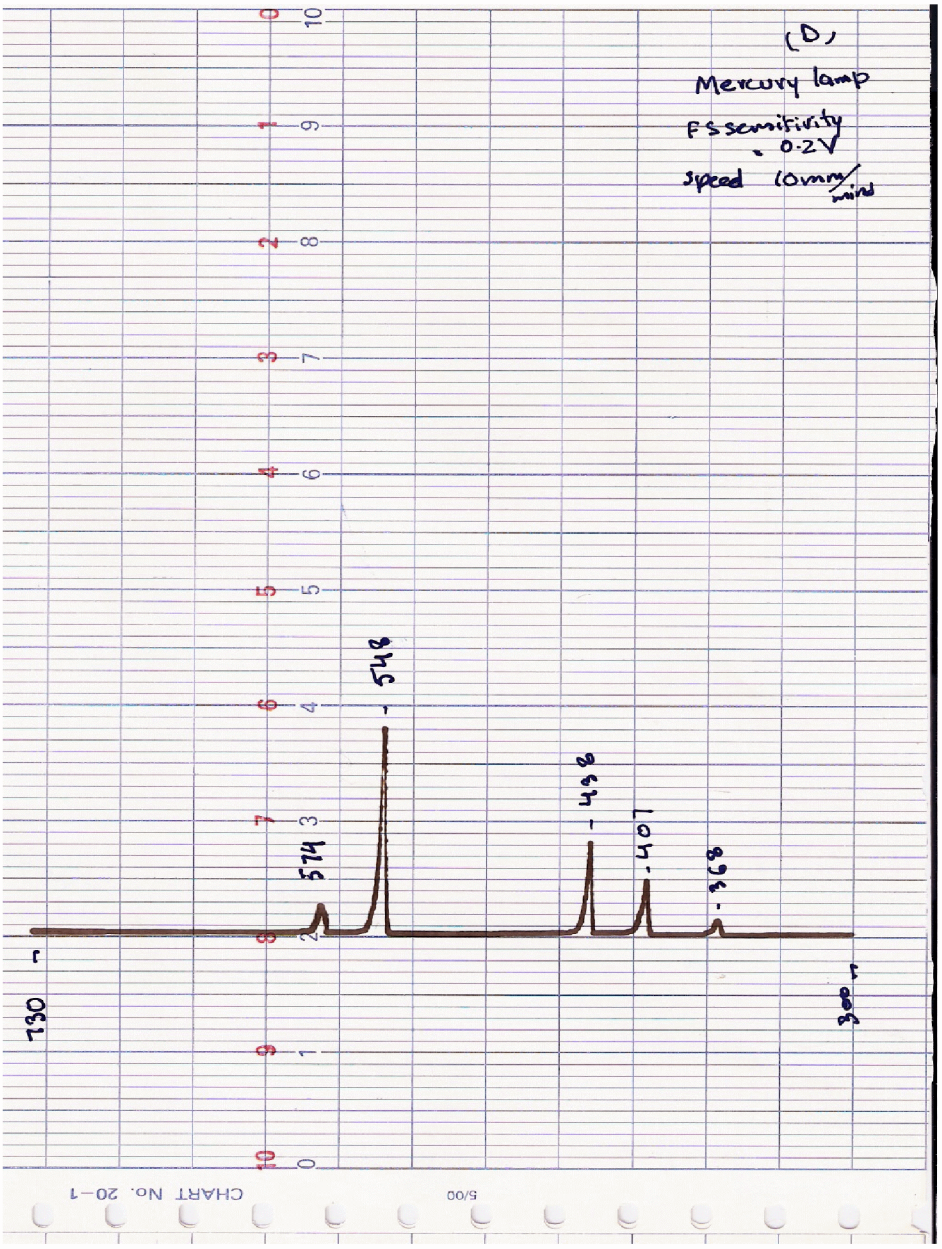

Fig (4.15): The mercury lamp spectrum for the wavelength range 300nm to 730nm

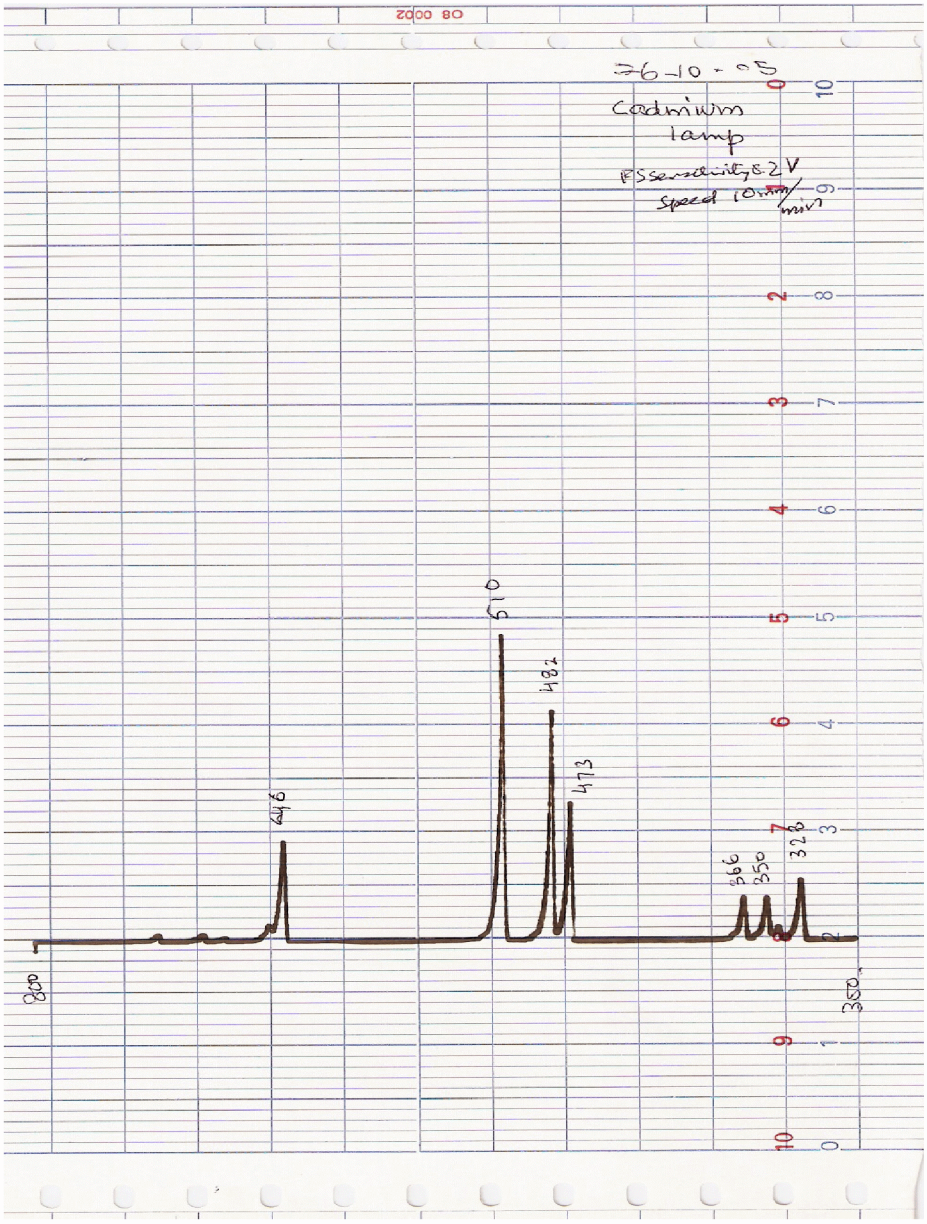

Fig (4.16): The cadmium lamp spectrum for the wavelength range 300nm to 800nm

Number of observations	Wavelength peaks Observed in experiment (nm)	Wavelength peaks by Young (nm)	Wavelength peaks by R-D-C (nm)
1	328		326
2	350		352
3	366		361
4	473	468	468
5	482	480	480
6	510	509	508
7	646		644

Table 4.1: Comparison of cadmium lamp wavelength peaks with the references

Number of observations	Wavelength peaks Observed in experiment (nm)	Wavelength peaks by Young (nm)
1	368	
2	407	405
3	438	436
4	548	546
5	574	577

Table 4.2: Comparison of mercury lamp wavelength peaks with the references

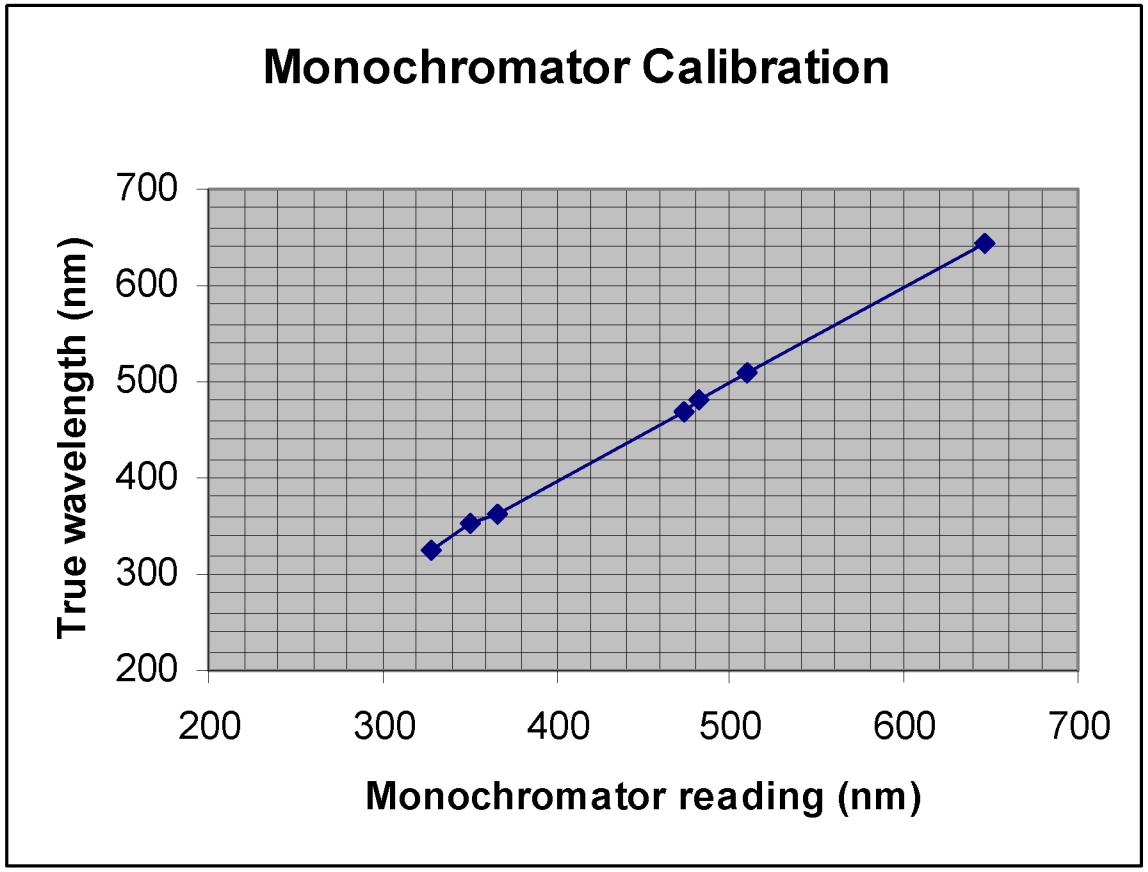

Fig (4.17): The monochromator calibration using cadmium lamp

4.5 Measurement of Optical fibre diameters

The samples from different types of optical fibres were studied under phase contrast microscope. Their core and cladding diameters were measured.

Type of Optical fibre	Core Diameter	Cladding Diameter
Optical fibre	10 μm	120 μm
Fibre core fibre	5 μm	125 μm
High Ge fibre	5 μm	120 μm
D-section fibre	10 μm	10 μm, 125 μm

Table 4.3: Measurement of optical fibre diameters

4.6 Measurement of Numerical Aperture

Numerical aperture is defined by

$$NA = n \sin \theta_{max}$$

Where θ_{max} is the angle of incidence for acceptance by the fibre.

4.6.1 Experimental Procedure

The optical fibre samples of about 2 meters in length were used for these experiments. The outer jacket of these fibre samples were removed about 5cm from both ends. A helium-neon laser was used for these experiments. Optical fibre samples were mounted on a rotation stage which could be tuned to setup launching of laser beam into the fibre sample at different angles. The radiations from helium-neon laser were launched into the optical fibre samples at different angles and corresponding output power was recorded using a power meter. The experimental setup is shown in figure (3.30). The power accepted by the optical fibre was measured as a function of the incident angle of laser beam. The plots were made for the power received by the detector as a function of sine of acceptance angle as shown in figures (3.31, 3.32 and 3.33) for different types of optical fibres. The full width of the curve was measured. Half-width of the curve at 5% of power received is the experimentally determined numerical aperture of the fibre. The value of critical wavelength was also measured for each type of optical fibre as given below.

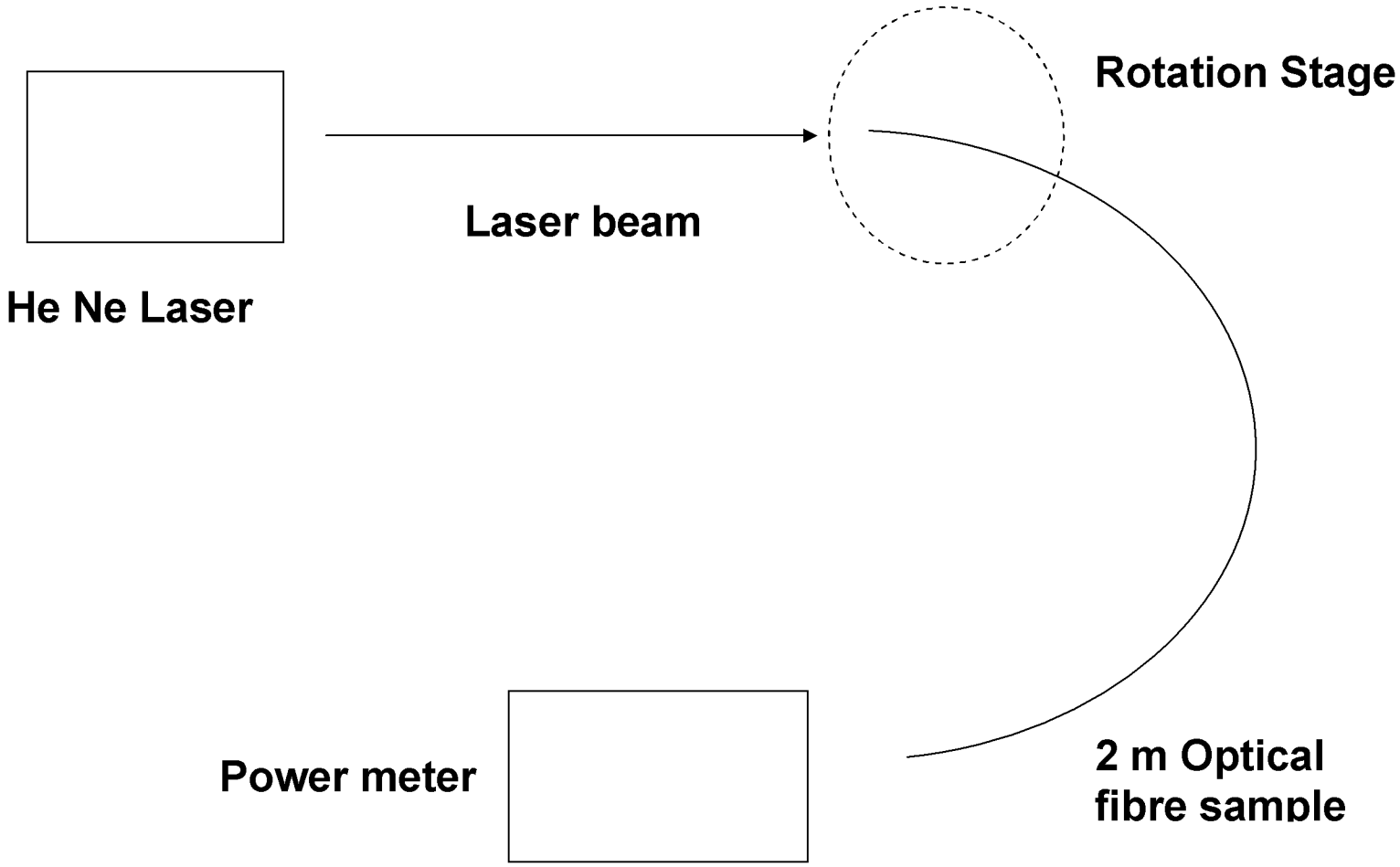

Fig 4.18 : Experimental Setup for NA measurement

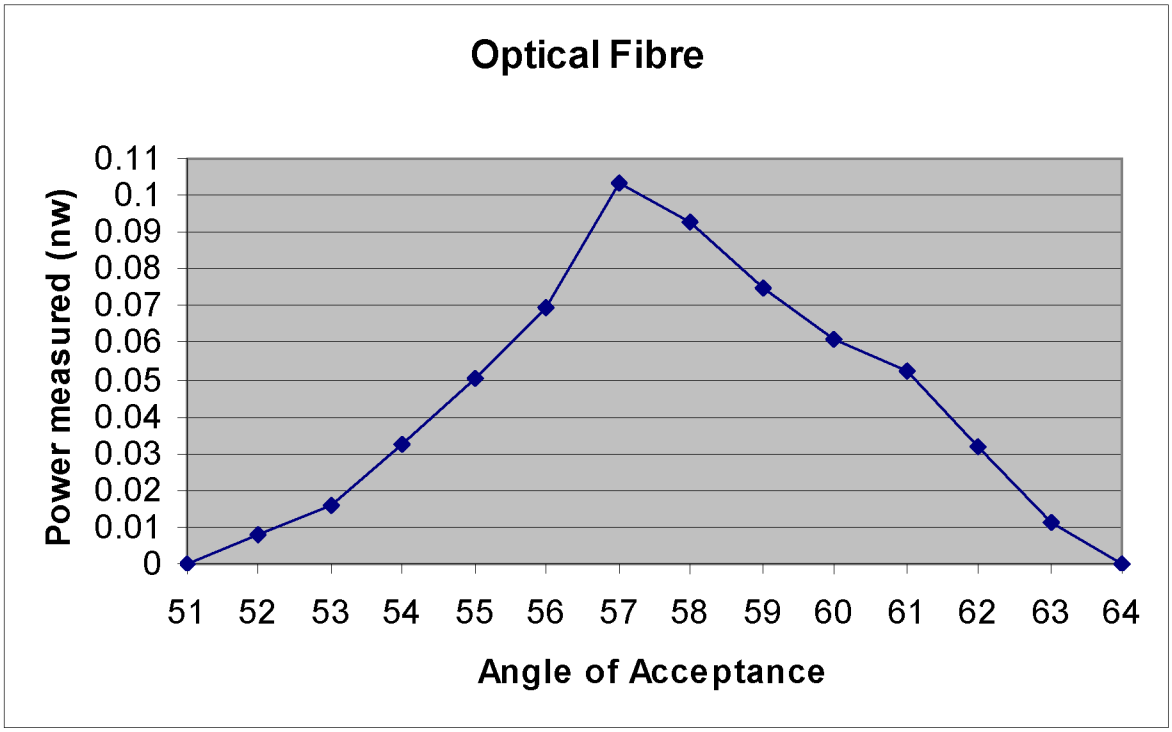

Fig (4.19): The plot of angle of acceptance by the optical fibre sample and output power measured

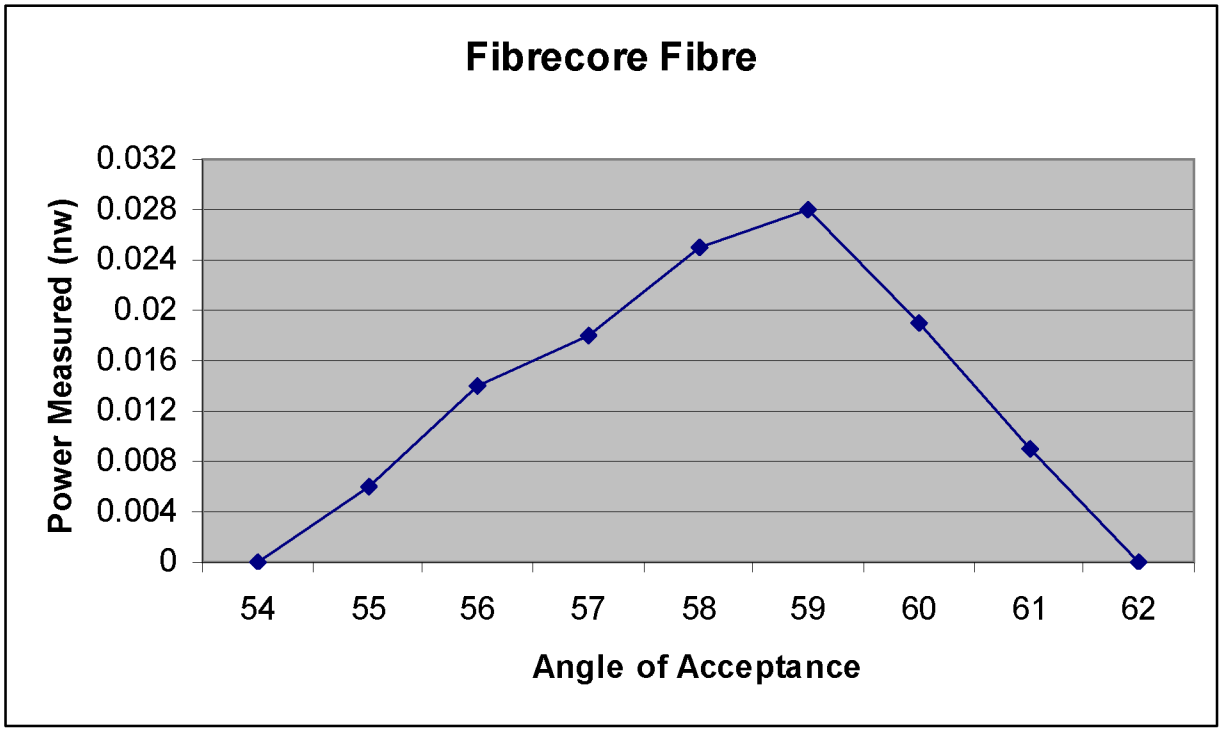

Fig (4.20): The plot of angle of acceptance by the optical fibre sample and output power measured

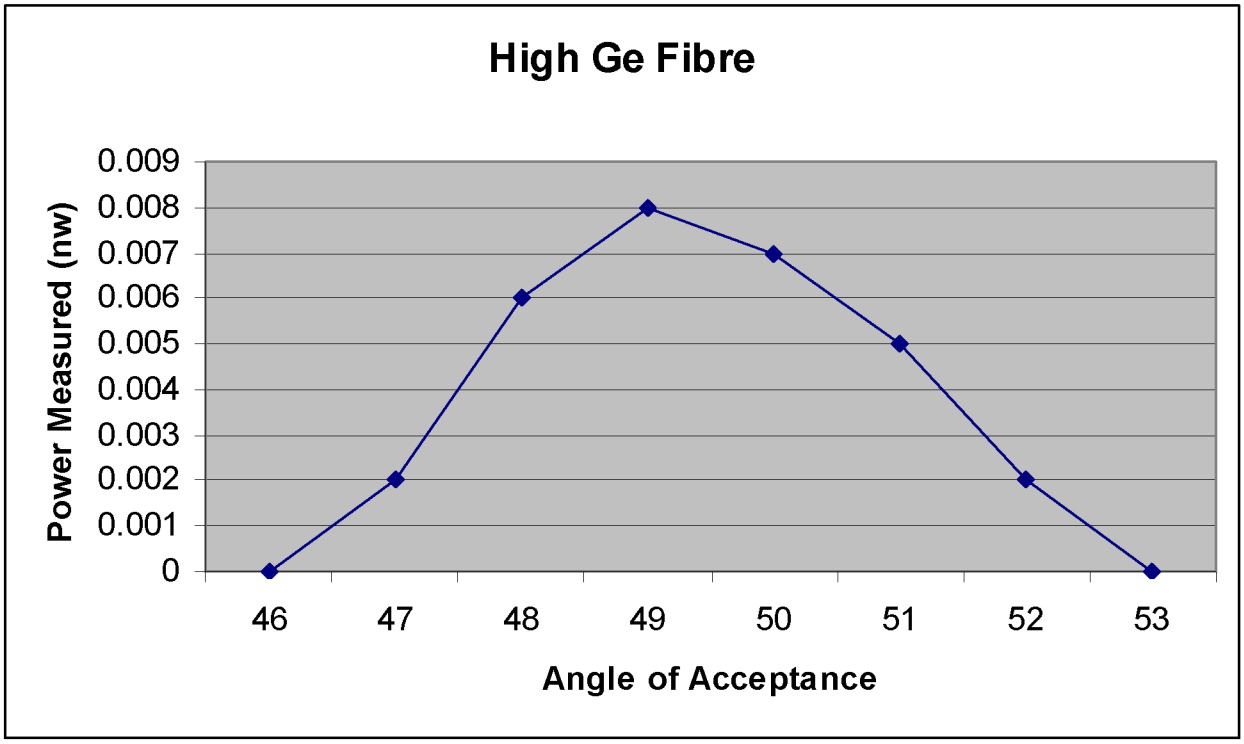

Fig (4.21): The plot of angle of acceptance by the optical fibre sample and output power measured

4.6.2 The Optical Fibre from Optical Fibre Company

The numerical aperture measurements for the optical fibre from Optical fibre company are as follows.

$2\theta_0 = 11.9$

$\theta_0 = 5.95$

$NA = Sin\theta_0 = 0.1$

$$\lambda_c = \frac{2\pi a \times NA}{2.4}$$

$\lambda_c = 1.3\mu m$

4.6.3 The Fibre core Fibre

The numerical aperture measurements for the optical fibre from fibre core company are as follows.

$2\theta_0 = 7.25$

$\theta_0 = 3.625$

$NA = Sin\theta_0 = 0.06$

$$\lambda_c = \frac{2\pi a \times NA}{2.4}$$

$\lambda_c = 0.39\mu m$

4.6.4 The High Ge Fibre from Nortel

The numerical aperture measurements for the high germanium optical fibre from Nortel company are as follows.

$2\theta_0 = 6.6$

$\theta_0 = 3.3$

$NA = Sin\theta_0 = 0.05$

$$\lambda_c = \frac{2\pi a \times NA}{2.4}$$

$\lambda_c = 0.65\mu m$

References:

1. F. G. Smith and T. A. King; Optics and photonics- An introduction, John Wiley and sons ltd, England, 2000.
2. A. S. L. Gomes, U. Österberg, J. R. Taylor; Spectral and Temporal Investigations of Nonlinearities in a non-Polarization preserving Single-mode Optical Fibre, Appl. Phys. B, 41, 235-240, 1986.
3. U. Österberg and W. Margulis; Experimental studies on efficient frequency doubling in glass optical fibres, Opt. Lett. 12, 57-59, 1987.
4. B.Valk, E. M. Kim and M. M. Salour; Second harmonic generation in Ge-doped fibres with a mode-locked Kr^{+} Laser, Appl. Phys. Lett. 51, 722, 1987.
5. F. Ouellette, K. O. Hill and D. C. Johnson; Enhancement of second harmonic generation in optical fibres by a hydrogen and heat treatment, Appl. Phys. Lett. 54, 1086-1088, 1989.
6. L. J. Wang, C. K. Hong and S.R. Friberg; Generation of correlated photons via four-wave mixing in optical fibres, J. Opt. B: Quantum Semiclass. Opt. 3, 346–352, 2001.
7. W. Keiser and G. C. B. Garrett; Two photons excitation in CaF, Phy Rev. Lett. 7, 229-231, 1996.
8. E. J. Woodbury and W. K. Ng; Ruby laser operation in the near IR, Proc. IRE. 50, 2367, 1962.
9. P. D. Maker, R. W. Terhune and C. M. Savage; Optical third harmonic generation in quantum electronics, Columbia University, New York, 1559-1578, 1964.
10. P. D. Maker and R. W. Terhune; Study of optical effects due to an induced polarization third order in electric field strength, Phys. Rev, 801-818, 1965.
11. K. I. White; Practical application of the refracted nearfield technique for the measurement of optical fibre refractive index profiles, Optical and Quantum Electronics, 11, 185-196, 1979.
12. S. Somekh and A. Yariv; Phase matching by periodic modulation of the nonlinear optical properties, Opt. Comm. 6, 301, 1972.

13. M. Froggat and T. Erdogan; All-fibre wavemeter and fourier-transform spectrometer, Optics Lett., 24, 942-944, 1999.
14. K. S. Lee and T. Erdogan; Fibre mode conversion with tilted grating in an optical fibre, J. Opt. Soc. Of Am. A., 18, 1176-1185, 2001.
15. D. Z. Anderson, V. Mizrahi and T. Erdogan; Production of in-fibre gratings using a diffractive optical-element, Elect. Lett., 29, 566-568, 1993.
16. X. M. Liu and H. Y. Zhang; Theoratical study for wavelength conversion of cascade second-order nonlinearity in silica fibre,International Journal of infrared and millimetre waves, 22, 1055-1064, 2001.
17. J. Stone; Interaction of hydrogen and dentrium with silica, J. Lightwave Technol, 57, 712, 1987.
18. K J. Plucinski, W. Gruhn, I. V. Kityk and S. Benet; Photoinduced second harmonic generation in Bi_2Se_3-$CaBR_2$-$PBCL_2$ optical fibres, Opt. Comm., 204, 355-361, 2002.
19. B. P. Antonyuk and V. B. Antonyuk; High efficient Second harmonic generation in Ge-doped silica fibres, Opt. Comm., 147, 143-147, 1998.
20. E. M. Dianov and D. S. Starodubov; Photoinduced Second harmonic generation in glasses and glass optical fibres, Opt. Fibre Tech., 1, 3-16, 1994.
21. G. Demouchy and G. R. Boyer; Growth rate of second harmonic generation in optical fibres, Opt. Comm., 101, 5-6, 1993.
22. E. J. Friebele, D. L. Griscom, and G. H. Sigel; Defect centres in a germanium-doped silica core optical fibre, Journal of Applied Physics, 45, 3424-3428, 1974.
23. E. J. Friebele, G. H. Sigel and D. L. Griscom; Drawing induced defect centres in a fused silica core fibre, Applied physics Letters, 28, 516-518, 1976.
24. G. N. Greaves; Colour centres in vitreous silica, Phil. Mag., 37, 447-466, 1978.
25. J. H. Mackey, JR; EPR study of impurity-related color centres in germanium-doped quartz, The journal of chemical physics, 39, 74-83, 1963.
26. E. A. Weaver, R. W. Heckman and E. L. William; Determining hydrogen diffusion in doped fused silica from the fluorescence, The journal of Chemical Physics, 47, 4891-4895, 1967.

27. P. J. Lemaire, R. M. Atkins, V. Mizrahi and W. A. Reed, High pressure H2 loading as a technique for achieving ultrahigh UV photosensitivity and thermal sensitivity in GeO2 doped optical fibres, Optics Letters, 29, 1191-1193, 1993.
28. M. C. Farries, P. St. J. Russell, M. E. Fermann and D. N. Payne; Second harmonic generation in an optical fibre by self written $\chi^{(2)}$ grating, Electron Letters, 23,322-324, 1987.
29. H. W. K. Tom, R. H. Stolen, G. D. Aumiller and W. Pleibel; Preparation of long-coherence-length second-harmonic-generating optical fibres by using mode-locked pulses, Optics Letters, 13, 512-514, 1988.
30. F. Ouellette, K. O. Hill and D. C. Johnson; Light-induced erasure of self-organised $\chi^{(2)}$ gratings in optical fibres, Optics Letters, 13,515-517,1988.
31. R. A. Myres, X. C. Long, S. R. J. Brueck and R. P. Tumminelli; Effect of hyhdrogen loading on temperature/electric-field poling of SiO_2 based thin films on Si, Optics Letters, 31, 1604-1606, 1995.
32. S. T. Huntingtin, K. A. Nugent, A. Roberts, P. Mulvaney and K. M. Lo; Field characterization of a D-shaped optical fibre using scanning near-field optical microscopy, J. Appl. Phys., 82, 510-513, 1997.
33. R. M. Ribeiro, L. R. Kawase, B. Lesche, B. Sahlgren, W. Margulis, R. Stubbe and K. Kleveby; All-optical control of bragg grating in semiconductor-coated D-shaped fibre, Optics Letters, 24, 454-456, 1999.
34. A. V. Kiryanov, V. Aboites and I. V. Melnikov; Enhancing type-II optical second-harmonic generation by use of a laser beam with a rotating azimuth of polarization, Apll. Phys. Lett., 78, 874-876, 2001.

Chapter 5

Spatial filtering in photo-chromic glasses

5.1 Introduction

The photochromic materials have been specified a place in between the photorefractive crystals and photographic materials due to their physical properties. Photochromics such as silver halide doped glasses and indolonospironaphthoxazines have shown to have limited diffraction efficiencies. Photochromes have a property of fading memory because of which they can be used as phase tracking devices. The photochromes are cheaper and widely available. Various studies have been done to investigate the processes underlying the phase grating process. Two coherent light beams have been shown to produce an interference pattern. Similar effects have been noticed in the photorefractive materials such as barium titanate and lithium niobate. In photorefractive materials two wave mixing takes place when the one of the

transmitted beams interacts with the first order diffracted beams. To achieve nonreciprocal energy transfer between the two laser beams a spatial shift between refractive index grating and the incident intensity pattern is required. A recognised method of causing spatial shift is by moving the gratings. Two-wave mixing is made possible by moving of the gratings.

The amplitude gratings created in the photochromic glasses have been observed to be in phase with the fringe patterns producing them therefore the photochromics do not create two wave mixing. By introducing dithering of the fringe pattern, there is possibility of achieving two wave mixing. The observation of diffracted beams on both sides of incident beam confirms the presence of a grating as a result of dithering. The transmitted power is modulated as a result of dithering of the fringe pattern. The modulation of the transmitted power is observed to be at twice the dither frequency. The amplitude of dither has been observed to affect the transmitted power.

5.2 Experimental Description

A He Ne Laser was used in experiments. A beam splitter was used to split the beam. One of the splitted beam passes through the photochrome glass and then through a microscope objective on to a BP × 65 photo diode. While the other splitted beam passes through the biprism, which was connected to a speaker to produce the dithering. This beam after going through the biprism passes through the photochrome glass and then through a × 5 microscope objective onto a photodiode.
The photodiode is connected to a lock-in amplifier. An xt-plotter was connected to the lock-in amplifier to record the results produced by the amplifier. The experimental setup is shown schematically in fig. 5.1.

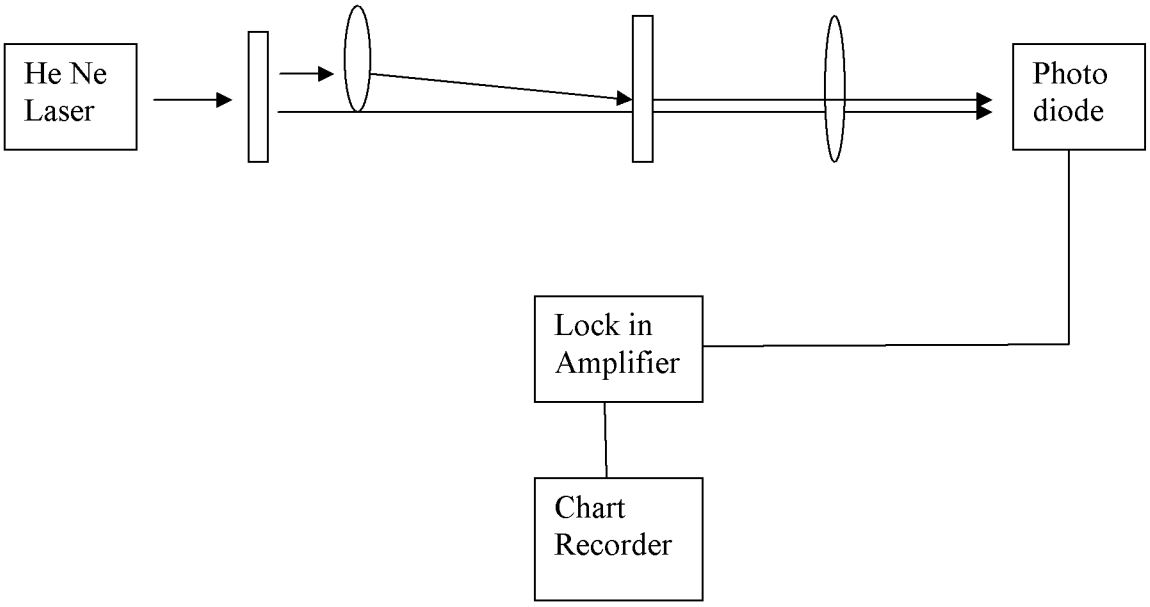

Fig (5.1): The experimental setup

5.3 Fourier Optics Applied to Amplitude/Phase grating with a pair of incident waves

When two beams of light overlap in the photochrome sample, interference is produced. As a result of this interference a refractive index grating is made inside the photochrome and diffraction is obtained.

The transmission coefficient of the grating formed can be written as

$$\tau(x) = \left[A - BCos\left[\frac{4\pi x}{d} \right] \exp\left[icSin\left(\frac{2\pi x}{d} + \frac{\pi}{2} \right) \right] \right]$$

Transmission coefficient consists of an amplitude component and a phase component. The first term in above equation gives amplitude term and second one is related with phase.

Let the sample is illuminated by monochromatic light of wavelength λ. The input electric field related to this beam can be written as

$$E_{in} = E_0 Cos\left[\frac{2\pi x}{d} + \phi(t) \right]$$

Where

$$\phi(t) = 2\pi\alpha Sin(\omega t)$$

The output electric field is given by

$$E_{out} = E_{in} \times \tau(x)$$

Submitting values in above equation we get

$$E_{out} = \left[A - BCos\left(\frac{4\pi x}{d} \right) \right] \exp\left[icSin\left(\frac{2\pi x}{d} + \frac{\pi}{2} \right) \right] E_0 Cos\left[\frac{2\pi x}{d} + \varphi(t) \right]$$

As we know

$$Exp\left[icSin\left(\frac{2\pi x}{d} + \frac{\pi}{2} \right) \right] = \sum_{n=-\infty}^{\infty} J_n(c) \exp\left[Sin\left(\frac{2\pi x}{d} + \frac{\pi}{2} \right) \right]$$

$$Exp\left[icSin\left(\frac{2\pi x}{d} + \frac{\pi}{2} \right) \right] = J_0(c) + J_1(c) 2iSin\left(\frac{2\pi x}{d} + \frac{\pi}{2} \right) + Higherterms$$

And

$$Cos\left[\frac{2\pi x}{d} + \phi(t) \right] = Cos\left(\frac{2\pi x}{d} \right) Cos[\phi(t)] - Sin\left(\frac{2\pi x}{d} \right) Sin[\phi(t)]$$

Furthermore

$$Cos[2\pi\alpha Sin(\omega t)] = J_0(2\pi\alpha) + \sum_{n=1}^{\infty} 2J_{2n}(2\pi\alpha) Cos(2n\omega t)$$

$$Sin[2\pi\alpha Sin(\omega t)] = \sum_{n=1}^{\infty} 2J_{2n-1}(2\pi\alpha) Sin[(2n-1)\omega t]$$

Substituting above formulae in equation 4.

$$E_{out} = \left[A - BCos\left(\frac{4\pi x}{d} \right) \right] \left[J_0(c) + J_1(c) 2iCos\left(\frac{2\pi x}{d} \right) \right] E_0 \times \begin{bmatrix} Cos\left(\frac{2\pi x}{d} \right) \left(J_0(2\pi\alpha) + 2J_2(2\pi\alpha) Cos(2\omega t) \right) \\ - Sin\left(\frac{2\pi x}{d} \right) 2J_1(2\pi\alpha) \sin(\omega t) \end{bmatrix}$$

$$E_{out} = E_0 \left[AJ_0(c) + 2iAJ_1(c) Cos\left(\frac{2\pi x}{d} \right) - BJ_0(c) Cos\left(\frac{4\pi x}{d} \right) - 2iBJ_0(c) Cos\left(\frac{2\pi x}{d} \right) Cos\left(\frac{4\pi x}{d} \right) \right]$$

$$\times \left[Cos\left(\frac{2\pi x}{d} \right) J_0(2\pi\alpha) + 2J_2(2\pi\alpha) Cos(2\omega t) Cos\left(\frac{2\pi x}{d} \right) - 2J_1(2\pi\alpha) Sin(\omega t) Sin\left(\frac{2\pi x}{d} \right) \right]$$

Thus

$$E_{out} = E_0\left[AJ_0(c)\left[J_0(2\pi\alpha) + 2J_2(2\pi\alpha)\cos(2\omega t)\right]\right]Cos\left(\frac{2\pi x}{d}\right) - 2AJ_0(c)J_1(2\pi\alpha)Sin(\omega t)Sin\left(\frac{2\pi x}{d}\right)$$

$$+\left[2iAJ_1(c) - BJ_0(c)\right]\left[J_0(2\pi\alpha) + 2J_2(2\pi\alpha)Cos(\omega t)\right]Cos\left(\frac{2\pi x}{d}\right)Cos\left(\frac{4\pi x}{d}\right)$$

$$-2iBJ_1(c)\left[J_0(2\pi\alpha) + 2J_2(2\pi\alpha)Cos(2\omega t)\right]Cos^2\left(\frac{2\pi x}{d}\right)Cos\left(\frac{4\pi x}{d}\right)$$

$$+4iBJ_1(c)J_1(2\pi\alpha)Sin(\omega t)Sin\left(\frac{2\pi x}{d}\right)Cos\left(\frac{2\pi x}{d}\right)Cos\left(\frac{4\pi x}{d}\right)$$

5.4 Amplitude of phase delay

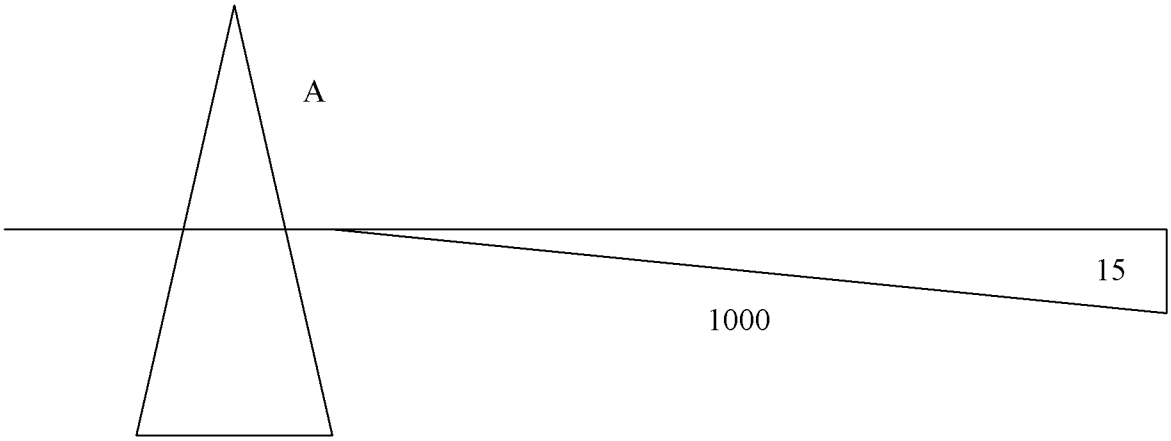

Fig (5.2): The Amplitude of phase delay

$$D = \frac{15}{1000}$$

$$A = \left(\frac{1}{\mu - 1}\right)\frac{15}{1000}$$

Where A is the prism angle and μ is the refractive index.

$$A = \frac{15}{0.5} \times \frac{1}{1000}$$

Amplitude of phase delay

$$= 0.5 \times A \times \frac{Amplitudeofosc}{\lambda} \times 2\pi$$

$$= \frac{0.5 \times 15}{0.5 \times 1000} \times \frac{25\mu m}{\lambda} \times 2\pi$$

Where (μ - 1) is the additional term due to dither of the prism.

$$A = 3.72rad$$

(Vsource)pp = 5v

(Source) rms = 1.77rad

For speaker oscillation measurement:

For 5v oscillation

500μm with R = 91Ω

For 1V oscillation

$$\frac{500}{5} = 100\mu m$$

For 1.8V (rms) oscillation

$$1.8 \times \sqrt{2} \times \frac{100 \times 91}{600} \mu m$$

Amplitude of phase delay =

$$2 \times \frac{0.5 \times 15}{0.5 \times 1000} \times \frac{38.6}{0.6328} \times 2\pi$$

$$= 5.75$$

For two beams = 5.75 × 2

= 11.5 rad

For 1.3V (rms) oscillation is

$$1.3 \times \sqrt{2} \times \frac{100 \times 91}{600} \mu m$$

= 27.88

Amplitude of phase delay =

$$2 \times \frac{0.5 \times 15}{0.5 \times 1000} \times \frac{27.88}{0.6328} \times 2\pi$$

= 4.15

For two beams = 4.15 × 2

= 8.31 rad

References:

1. R. J. Potton; Adaptive spatial filtering using photochromic glass, Meas. Sci. Technol. 10, 1315-1318, 1999.
2. M. Z. Zha and P. Gunter; Nonreciprocal optical transmission through photorefractive KNbO3:Mn, Opt. Lett. 10 (4), 184-186, 1985.
3. M. Z. Zha, and P. Gunter; Measurement of phase shift of photorefractive gratings by a novel method, IEEE journal of quantum electronics, 26(4), 788-792, 1990.
4. Oliveira, J. Frejlich, L. Arizmendi and M. Carrascosa; Holographic phase shift measurement during development of a fixed grating in lithium niobate crystals, Opt. Lett. 28 (12), 1040-1042, 2003.
5. K. Macdonald, J. Feinberg, M. Zha and P. Gunter; Asymmetric transmission through a photorefractive crystal of barium titanate, Opt. Comm. 50 (3), 146-150, 1984.
6. I. McMichael and P. Yeh; Phase shifts of photorefractive grating and phase-conjugate waves, Opt. Lett., 12, 48-50, 1987.
7. Lahiri, L Pyrak-Nolte, D. Notle and M. Melloch; Transient dynamics during two-wave mixing in photorefractive quantum well diodes using moving gratings, Opt. Express. 2 (11), 432-438, 1998.
8. L. J Wang, C. K. Hong and S. R. Friberg; Generation of correlated photons via four-wave mixing in optical fibres, J. Opt. B: Quantum semiclass Opt. 3, 346-352, 2001.
9. P. Gunter; Holography, coherent-light amplification and optical-phase conjugation with photorefractive materials, Phys. Rep., 93, 199-299, 1982.
10. A. N. Vaslov and T. M. Antonsen; Numerical solution of fields in lossy structured using MAGY, IEEE Trans Electron devices, 48, 45-55, 2001.
11. He P; Simulation of ultrasound pulse propagation in lossy media obeying a frequency power law, IEEE Trans Ultrasonics, Ferroelectrics and frequency and frequency control, 45, 114-125, 1998.
12. D. R. Penn and M. D. Stiles; Solution of the Boltzmann equation without the relaxation-time approximation, Phys Rev D, 59, 13338-13346, 1999.

13. P. St J. Russell; Interference of integrated Floquet-Bloch waves, Phys Rev A, 33, 3232-3242.
14. M.Carvalho, A. Grandpierre, D. Christodoulides and M.Segev; Optical spatial shock waves in photorefractive media, Physical review, 62, 8657-8662, 2000.
15. D. D. Keck, R. D. Maurer, and P. C. Schultg; On the ultimate lower limit of attenuation in glass optical waveguide, Appl. Phys. Lett., 22, 307-309, 1973.
16. N. shibata, M. Kawachi, and T. Edahiro; Optical loss characteristics in high GeO_2 content silica fibres, Tran. IECE Japan, E63, 837-841, 1980.

Conclusions

The photosensitivity of the optical fibres and the effects arising as a result of this photosensitivity were studied and presented. The aim of this work and research done here was to study in more detail the reasons behind the nonlinear effects observed in optical fibres because of this photosensitivity.

In this chapter the achievements laid out in this thesis, and the way forward, will be summarised. There have been several interesting developments that point the way to a large expansive field of work. The overall theme was set out in chapter one, pointing out the possibilities of optical fibre photosensitivity, which includes second harmonic generation and fibre Bragg gratings. Each chapter then approached the theme from a different perspective. In chapter two, theoretical predictions of photo induced index changes from different wavelengths or intensity was demonstrated, though the results were not really clear-cut. Changes due to unlike photons were observed by using both UV and Nd: YAG as pump radiation. While in chapter three the experimental work done was described and the output explained. In chapter four, the effects of hydrogen on a standard and highly photosensitive were demonstrated. Increased loss and photosensitivity is a notable effect. Chapter four was centred not only on producing SHG from fibres, but what factors (endogenous and exogenous) affects this process. Chapter five focused on spatial filtering in photo chrome materials.

The origin of parametric processes, classified as second-order or third-order processes depending on order of susceptibility, lies in the nonlinear response of a material to an applied optical field. The second-order susceptibility $\chi^{(2)}$ vanishes for Centro-symmetric material such as silica fibres, however in practice these processes are reported to occur. Four wave mixing (FWM) in optical fibres has been studied extensively since it can be quite efficient in generating new waves.

A Q-switched and mode-locked 1.06μm Nd: YAG laser was used to study short fibre samples 20-50 cm while a Q-switched 1.06μm Nd: YAG laser was used to carry out experiments with long optical fibre samples of about 1.5km. Along with second harmonic radiation at 532nm

other wavelengths at 355nm, 585nm, 647nm, 709nm and 820nm have also been observed in spectrum from the irradiated fibre samples.

The 647nm wavelength, also reported in past study by Taylor et al, has been attributed to the four-wave mixing mechanism with the fundamental wavelength acting as the pump wave. The 355nm wavelength is recognised as the third harmonic of fundamental 1.06μm wavelength.

The spectra recorded provide clues about the colour centres that make the fibres sensitive to light. Several models have been used to understand the second harmonic generation process. SHG is stated to be result of periodic ordering of color centres or defects along the fibre in such a way that the phase matching is automatically satisfied. However there is a possibility that $\chi^{(3)}$ susceptibility results in SHG as it is an allowed effect therefore excluding the breaking of inversion symmetry in the optical fibre core.

Second harmonic generation in specimens of several different types of single mode optical fibre has been observed. Different lengths of optical fibres, with different dimensions and different characteristics, were used in the experiments. What is new is that second harmonic generation has been observed in the D-section fibre. The D-section fibre differs in its structure from normal single mode fibre, as its cladding is not circularly symmetric rather it has a D-shaped cladding. The basic reason for using the D-section fibre was to reduce the hydrogen diffusion time; however it showed a number of different characteristics. The waveguiding properties of D-section fibres are different from those of normal fibres with strong waveguiding dispersion and scattered modes output resulting from its non-symmetric structure.

Along with SHG some other nonlinear optical processes taking place inside optical fibre were also observed. It has been observed that Resonance enhancement of nonlinear processes and multiphoton absorption is involved in up conversion of infrared laser pulses to visible in optical fibres.